arXiv:2611.15744v1 [cs.LG] 11 Nov 2026

Latent Imagination for Parameterized Action Spaces

Atahan Cilan [1] **İhsan Mert Muhacıroğlu** [1] **Ümit Can Bekar** [1]

Abstract

Parameterized-action MDPs (PAMDPs) ask an agent to choose a discrete action together with continuous parameters whose meaning depends on that choice. Model-free PAMDP methods act fast but need many interactions; model-based methods are sample-efficient but plan at every decision, which makes them slow to act. We introduce HyLI (Hybrid Latent Imagination), a model-based agent that learns a hybrid policy entirely in the latent imagination of a world model and acts with a single forward pass. To address learning problems that the PAMDP structure creates, HyLI adds counterfactual mode evaluation, which gives every discrete action a learning signal at every imagined state, and success-window replay, which keeps rare successes in training. On seven standard PAMDP benchmarks, HyLI is within one published standard deviation of, or above, the published score of the strongest model-free baseline in our comparison on all 7 tasks, reaches 90% of that score with 2.4× fewer environment steps than that baseline (5.0× when its reward-free pre-training is counted), and decides 67× faster than the model-based planner DLPA at its published planner settings. It is the only method in our comparison that is both more sample-efficient than that baseline and fast enough for real-time control.

1. Introduction

Many real-world control problems combine a discrete choice with continuous parameters. A robot selects a manipulation primitive and its arguments (Dalal et al., 2021; Nasiriany et al., 2022) (Figure 1a) or switches between control modes (Neunert et al., 2020); an automated vehicle decides whether to change lanes and how (Lin et al., 2024); a UAV chooses between moving and turning and sets the acceleration or the turn angle (Feng et al., 2023); a game agent selects a skill and where to aim it (Xiong et al., 2018). Parameterized-action MDPs (PAMDPs) formalize this structure (Masson et al., 2016): at each step the agent chooses a mode $k \in \{1, \dots, K\}$ and a parameter $x_k \in \mathbb{R}^{d_k}$ whose dimension and meaning may differ from mode to mode. Flattening the hybrid space into a purely discrete or a purely continuous one—discretizing the parameters or relaxing the mode—either loses precision or lets the agent mix incompatible actions. PAMDP algorithms are developed and compared on a common suite of simulated benchmarks, from robot soccer and a platform game to multi-actuator navigation tasks (Masson et al., 2016; Hausknecht & Stone, 2016; Li et al., 2022).

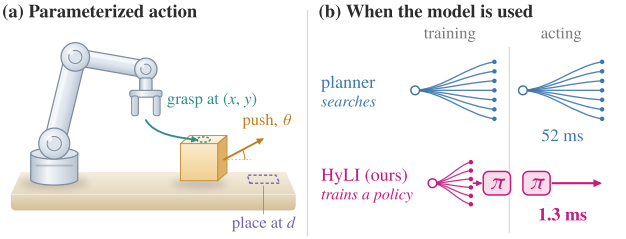


Figure 1. **(a)** A parameterized action: the robot chooses a primitive (mode) and its arguments (parameter), whose meaning differs from primitive to primitive. **(b)** Both kinds of agent roll out a learned model. A planner uses the rollouts to search for an action at every decision, during training and when acting. HyLI uses them only during training, to train a policy π, and acts with one forward pass of π. Times: median per decision on one CPU thread, Goal benchmark (all tasks in Table 2).

Model-free PAMDP methods (Xiong et al., 2018; Fan et al., 2019; Li et al., 2022) act with a single forward pass of their networks but need many interactions. The model-based methods, DLPA (Zhang et al., 2024) and FLEXplore (Wang et al., 2025), learn a dynamics model and report large gains in sample efficiency, but they select every action by planning (Figure 1b): thousands of candidate sequences are rolled through the model per decision, and the cost grows with the planning horizon and, in the released implementation, with the number of modes. Diffusion policies such as CHDP (Liu et al., 2026) run denoising chains per decision. Many of the applications above, however, run in a control loop at tens to hundreds of decisions per second.

We ask whether a model-based PAMDP agent can keep

[1]Turkish Aerospace. Correspondence to: Atahan Cilan <atahan.cilan@tai.com.tr>.

Preprint. November 13, 2026.

the sample efficiency of a learned model without searching at decision time. World-model agents in the Dreamer line (Hafner et al., 2025) learn a policy inside imagined latent trajectories and act with one forward pass. Carrying this to PAMDPs is not a matter of swapping the action head, because a PAMDP is two coupled but structurally different learning problems: the discrete choice has no unbiased pathwise gradient, and the continuous choice can be differentiated through the model only along the mode that was sampled, so a rarely chosen mode's parameters are rarely trained and can starve.

We propose HyLI (Hybrid Latent Imagination), which learns a hybrid mode-and-parameter policy in imagination and gives each half of the action its own gradient estimator. To keep rarely chosen modes learning, counterfactual mode evaluation (CME) values every candidate mode with one imagined step; to keep rare successes in training, success-window replay (SWR) draws part of every batch from windows that contain one. Our contributions are:

- HyLI (Section 3), to our knowledge the first agent to bring latent imagination to the standard PAMDP benchmarks with a separate gradient estimator for each half of the action and counterfactual mode evaluation, compared there against planners. It acts with one forward pass of its policy, with one configuration whose per-task switches follow fixed rules, on tasks with 2 to 256 nominal modes. It is within one published standard deviation of, or above, the published score of the strongest model-free baseline in our comparison on all 7 tasks, reaches 90% of it with 2.4× fewer interactions (geometric mean; 5.0× with its reward-free pretraining counted) and decides 67× faster than DLPA at its published settings (Section 4.2): a balance of sample efficiency, final performance and decision speed that neither the model-free methods nor the planner reach.
- Counterfactual mode evaluation (Section 3.3), which trains the mode head with an expected policy gradient and gives every parameter head a gradient whether or not its mode was sampled. Along the cumulative ablation, it and SWR account for most of the gain on the two sparse-success tasks (Section 4.3).
- A detailed analysis of actor designs for PAMDPs: a cumulative and a leave-one-out ablation, the direct adaptation of DreamerV3 with a relaxed continuous actor, and a comparison of shared and per-mode parameter heads that measures cross-mode gradient interference and its effect on performance (Sections 4.3 and 4.4). All experiments follow a reproducible protocol: every baseline runs from its official code (agents unchanged, drivers ported), every environment interaction is counted, and all methods are scored on the same window of interactions (DLPA at its shorter converged budget; Section 4.1, Appendices A and E). Code will be released.

2. Background

PAMDPs. The action space of a PAMDP (Masson et al., 2016) is $\mathcal{A} = \bigcup_{k=1}^{K} \{(k, x_k) : x_k \in \mathcal{Z}_k \subseteq \mathbb{R}^{d_k}\}$. The dimension d_k may differ across modes (in Goal, a kick takes a 2-D target and each shot a 1-D target position on the goal line), and so may the *semantics* of x_k: in Goal the parameters of different modes are different physical quantities (*heterogeneous*), whereas in Hard Move all 2^n modes take the same scalar thrust (*homogeneous*).

Latent imagination. DreamerV3 (Hafner et al., 2025), the latest agent of the Dreamer line (Hafner et al., 2019; 2020; 2021), learns a recurrent state-space model (RSSM) with deterministic state h_t and categorical stochastic state $\mathbf{z}_t$ from replayed sequences. An actor and a critic are trained purely on trajectories imagined by the model; the critic regresses λ-returns and the actor maximizes normalized returns plus an entropy bonus. At deployment only the encoder, the recurrent core and the actor run. We change the action interface, the actor and its gradient estimators; the world model and critic follow DreamerV3 with reduced sizes, re-implemented in PyTorch (Appendices B and E.1).

Planning in PAMDPs. DLPA (Zhang et al., 2024) learns hybrid-action-conditioned dynamics, reward and termination models and selects each action by MPPI (Williams et al., 2017): for I iterations it samples N sequences of length L, each step a mode and a per-mode Gaussian parameter, rolls them through the model and refits the sampling distributions. With the published settings (I=6, N=1000, $L \in \{5, 8, 10\}$) one decision costs $I \cdot N \cdot L = 30\,000$–$60\,000$ model steps. This count does not depend on K; the released implementation, however, loops over the modes serially (Appendix E), so its decision time also grows with K.

3. Method

Figure 2 gives an overview of HyLI, from acting to training. The world model is a DreamerV3 RSSM whose action input encodes the hybrid action; the actor has a discrete mode head and per-mode parameter heads (Section 3.1), trained in imagination with a different gradient estimator for each half (Section 3.2) and with counterfactual mode evaluation (Section 3.3). Nothing in Sections 3.2 to 3.4 runs at deployment.

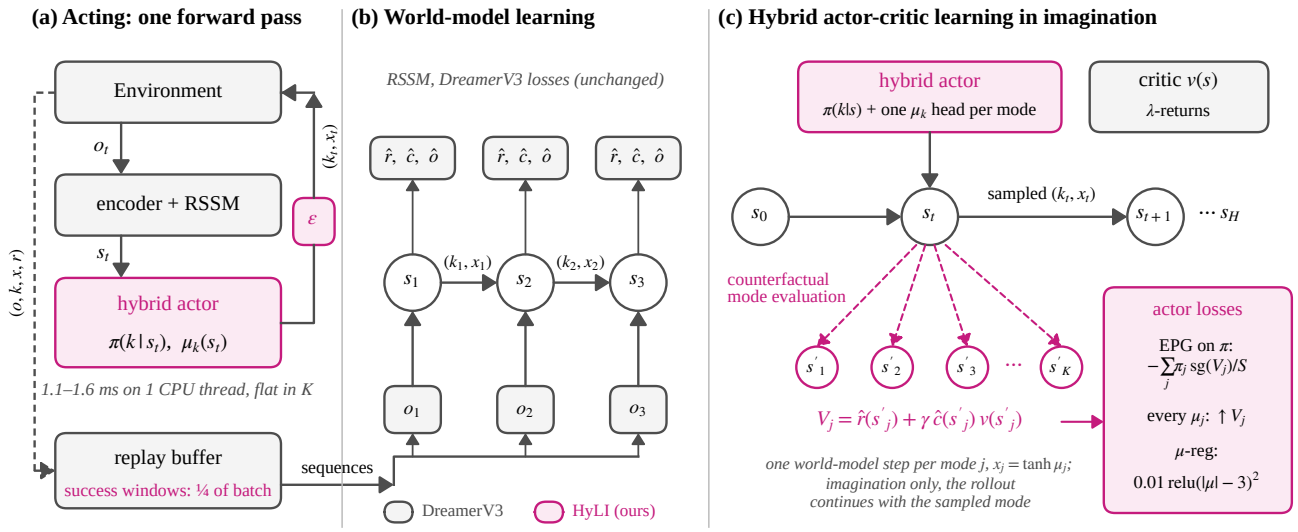


Figure 2. Overview. **(a)** Acting is one forward pass through the encoder, the recurrent core and the hybrid actor; on Goal and Hard Goal the mode is occasionally replaced by a uniform one early in training (ε). **(b)** The world model is a DreamerV3 RSSM trained on replayed sequences, a quarter of each batch drawn from windows that contain a success (SWR). **(c)** The actor and critic learn on imagined rollouts that continue with the sampled mode. From every imagined state, CME (dashed) takes one model step per candidate mode j and values it, V_j; the values train the mode head by the expected policy gradient and every parameter head by its own V_j. Magenta: parts that HyLI adds for PAMDPs; grey: unchanged DreamerV3 components.

3.1. Hybrid actor

The world model receives $[\,\mathrm{onehot}(k) \mid x_1 \mid \ldots \mid x_K\,]$ with every slice but the selected mode's set to zero, so no two modes alias an input unit; on Hard Move, where every mode has the same single parameter, the smaller $[\,\mathrm{onehot}(k) \mid x_k\,]$ is equivalent (Appendix A.1). The actor maps the latent feature $s = (h, \mathbf{z})$ to a categorical $\pi(k \mid s)$ (1% uniform mixing) and, per mode, a Gaussian over pre-squash parameters with mean $\mu_k(s)$; the executed parameter is $\tanh$ of a sample. The parameter head is either `sub`, one MLP per mode (no cross-mode interference by construction), or `multi`, a shared trunk with one output row per mode.

Whether the parameter heads should share weights is not obvious. When the parameters of different modes are different physical quantities, an update that improves one mode's parameter (a kick target) can disturb another's (a shot position) through a shared trunk, a form of gradient interference; when they are the same quantity, sharing may instead help. To measure how this choice affects performance, we implement both heads and compare them in Section 4.4. By default we use `multi` where every mode has the same single parameter (Hard Move) and `sub` on the other tasks.

3.2. Split gradient estimators

The continuous half is differentiable through the model: the parameter loss is the negative normalized λ-return, backpropagated through the imagined dynamics as in DreamerV3's continuous control; in this term the critic's bootstrap values are detached, so the gradient flows through the predicted rewards and continuations (Appendix B). The discrete half has no unbiased pathwise gradient (straight-through and Gumbel-softmax estimators (Bengio et al., 2013; Jang et al., 2017) are biased). Without CME it is trained with the score-function estimator $-\log \pi(k_t \mid s_t)\, \mathrm{sg}(A_t)$, with stop-gradient sg and advantage A_t, the normalized λ-return minus the critic's value; in the full method CME replaces this estimator by an expected policy gradient (Section 3.3), so the score-function estimator is used only in the first rows of the ablation ladder (Section 4.3). In both cases the one-hot of the sampled mode enters the world model *detached*, so the return gradient does not reach the mode logits a second time through a relaxed one-hot. Both halves carry an entropy bonus of $3 \cdot 10^{-4}$ on every task; for the parameters it is the entropy of the selected mode's pre-squash Gaussian.

3.3. Counterfactual mode evaluation

The score-function estimator learns from the one mode that was sampled, and the pathwise gradient improves that mode's parameters only. A rarely sampled mode is rarely improved, can look worse and be sampled even less. CME is designed to break this loop with the world model we already have. At every imagined state s_t and for each of the C candidate modes j (the set is defined below) we take one imagined step with that mode and its deterministic parame-

ter,

$$s'_j = f\big(s_t,\ (j, \tanh \mu_j(s_t))\big),$$
$$V_j = \hat{r}(s'_j) + \gamma\, \hat{c}(s'_j)\, v(s'_j), \tag{1}$$

where f is one step of the RSSM prior (one sample) and $\hat{r}$, $\hat{c}$ and v are the existing reward, continuation and critic heads. Because the parameter is the mean, V_j is a biased estimate of the mode's value under the stochastic policy. The imagined trajectory still continues with the sampled mode, so the extra cost is $H \cdot C$ one-step evaluations per start state, not a tree. The values are used twice: the mode head receives, in place of the score-function estimator, the expected policy gradient (Ciosek & Whiteson, 2018) $-\sum_j \pi_j \operatorname{sg}(V_j)/S$, which has zero variance in the mode choice (S: DreamerV3's return scale, Appendix A.2); every candidate's parameter head ascends its own value, $-\frac{1}{C}\sum_j V_j/S$, whether or not the mode was sampled. This term differentiates through v but does not update the critic. With `sub` heads, the pathwise term reaches mode j's parameters only when j is sampled, with weight $\pi_j(s_t)$ in expectation; this term gives every candidate weight $1/C$, so the heads stay isolated and every candidate is trained at every imagined state. The sampled mode's parameters receive this gradient and the pathwise one with equal weight. The candidate set is all modes when $K \le 16$; otherwise the 8 most probable plus 8 drawn uniformly without replacement from the rest, with π renormalized over the set, a biased approximation whose cost does not grow with K.

3.4. Replay, exploration and regularization

Three single-switch components target failures we observed on Goal and Hard Goal, where a random policy almost never scores; Section 4.3 adds and removes them one at a time. Success-window replay (SWR) draws a quarter of every batch from windows that contain a success event (on the MPE tasks, a step with reward above 4, the success rule of the benchmark), so that rare early successes are not diluted; it is a simple form of prioritized replay (Schaul et al., 2016), close in spirit to self-imitation learning (Oh et al., 2018). Intuitively, SWR keeps successful experience in view: the world model, and the imagined rollouts the actor learns from, continue to represent success while it is still rare. ε-mode exploration replaces the policy's mode by a uniform one with a probability that decays from 0.1 to 0 over the first $5 \cdot 10^4$ steps after the prefill; only the replay data change. Finally, a $\tanh$-squashed parameter whose mean saturates receives almost no gradient and can stay at its bound, a failure that Hausknecht & Stone (2016) documented for PAMDPs and prevented by inverting gradients near the bounds. We use a simpler penalty: μ-regularization adds $0.01 \cdot \mathrm{relu}(|\mu_k| - 3)^2$ to the actor loss, on the bounded mean (Table 6), which is zero for $|\mu| \le 3$ and pulls a saturating mean back. Replay, imagination and prefill details are in Appendix A.2.

4. Experiments

We first compare HyLI with all baselines on final score, decision time and sample efficiency (Section 4.2), then study its components (Section 4.3) and the design of its parameter head (Section 4.4).

4.1. Protocol

Tasks, arms and scores. We use the PAMDP suite of Li et al. (2022): Platform, Goal, Hard Goal, Catch Point and Hard Move, $n \in \{4, 6, 8\}$, the last two built on the multi-agent particle environment (MPE) (Lowe et al., 2017), with K from 2 modes on Catch Point to 256 on Hard Move (n=8) (Table 12). We call each compared method an *arm* and each arm–task pair a *cell*. The baselines P-DQN (Xiong et al., 2018), PA-TD3 (Hausknecht & Stone, 2016; Li et al., 2022), HHQN (Fu et al., 2019), H-PPO (Fan et al., 2019) and HyAR (Li et al., 2022), all but H-PPO in their TD3 variants (Fujimoto et al., 2018), run the reference agents unchanged with ported drivers and their per-task settings; the released HHQN-TD3 differs from TD3 in ways we keep (Appendix D.2). DLPA is ported from its official code and verified bit-exact against it; P-DQN keeps its hand-coded parameter prior on Platform and Goal. Every baseline runs with the per-task settings its authors published for these tasks, without re-tuning; while adding our components we tried variants on every trained task except Hard Move (n=8), mostly on Goal and Hard Goal, then fixed one configuration for every experiment; Hard Move (n=8) was not used to choose any component or setting. Every arm is trained with the same five seeds (0–4) on every task. A run's score is the mean of its final five evaluations (100 greedy episodes each, in a separate environment); the metric is the reference one, return on Platform and success rate elsewhere. Every environment interaction counts, HyAR's reward-free pre-training included, and all arms are scored on the same window: their first B interactions, B our budget on the task (DLPA at its shorter converged budget). DLPA plans at every training step, so a run at the reference budget would take one to several weeks per seed. It runs at the budget of its own paper; where it is not within one published standard deviation of its published return there, we extend the run until it converges. Details and every deviation from the reference code: Appendices A and E.

Metrics. Sample efficiency is the number of environment steps a run needs to first reach 90% of HyAR's published score (median over seeds; a seed that never reaches it is censored at its budget). We compare decision rates against 50 Hz, a common rate for learned low-level control on physical systems: legged robots run their learned policies at 50 Hz (Rudin et al., 2022) and 200 Hz (Hwangbo et al., 2019), and autopilots typically sample at 100 Hz (Bøhn et al., 2019). A racing agent that competes against humans

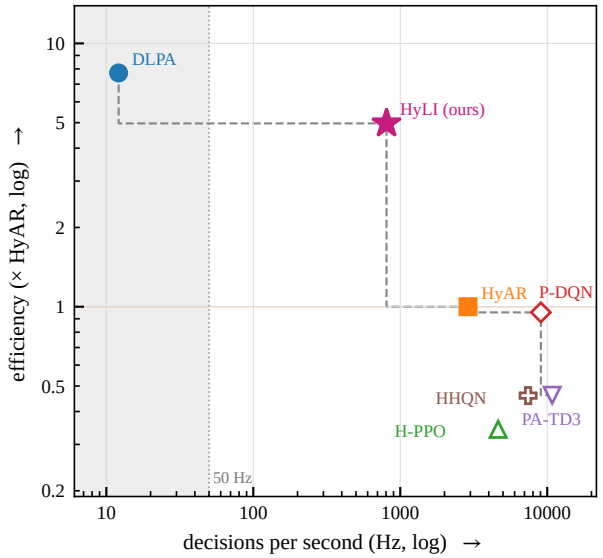


Figure 3. Sample efficiency against decision rate, both higher-is-better. x: decisions per second on one CPU thread (Table 2 and Table 19). y: HyAR's steps to the threshold, pre-training included, divided by the arm's (Table 3), geometric mean over tasks; open markers are upper bounds (a task median is censored). Shaded: below 50 Hz. Dashed: Pareto front. Per task: Appendix F.

in real time in a driving simulator acts at 10 Hz (Wurman et al., 2022), so we also state the result at 10 Hz.

4.2. Results

Final score. HYLI has the highest mean on 5 of the 7 tasks (Table 1) and no failing seed. The exceptions are Hard Move (n=4), where HyAR is ahead within the window, and Hard Move (n=8), where DLPA is. Against the published results of Li et al. (2022) it is within one published standard deviation or above on all 7 tasks and more than one above on 3 (Platform, Hard Goal and Catch Point). CHDP reports higher success on Goal, Hard Goal and Hard Move (n=4) under its own protocol; without released code we do not rank against it (Appendix C). Goal and Hard Goal separate the arms: HHQN and H-PPO stay near zero success on both and PA-TD3 on Goal, at the deceptive optimum of shooting from the start position, and some DLPA seeds lock into the same optimum and never leave it.

Decision time. One decision of HYLI takes 1.1–1.6 ms on one CPU thread (at least 640 Hz on every task, Table 2). DLPA is 67× slower (geometric mean over the seven trained tasks) and reaches at most 22 Hz, 33 Hz on a GPU, and even a 10 Hz loop excludes it on Platform, Hard Move (n=8) and Hard Move (n=10). The cost of every policy stays nearly flat from K=2 to K=1024, whereas the released planner's grows with its horizon and, because it loops over modes serially (Appendix E), with K, from 40× to 286× ours on the trained tasks and to 1145 ms on Hard Move (n=10). The model-free policies are 3 to 17× faster than ours. The extra computation of HYLI is paid during training instead: CME multiplies the update time by 1.4 to 2.6 (Appendix B).

Sample efficiency. Figure 3 summarizes the trade-off. The model-free arms decide fastest, but none is more sample-efficient than HyAR in geometric mean, and several never reach the threshold. Counting only arms whose five seeds all reach the threshold (Table 3), DLPA needs the fewest interactions on 5 of the 7 tasks; at its published planner settings it decides below 50 Hz on every task. HYLI lies on the front between them and is the only arm both above 50 Hz and more sample-efficient than HyAR: 2.4× fewer steps than HyAR without its reward-free pre-training (geometric mean; 1.4× to 5.8× per task) and 5.0× with it. By the same count it is the most sample-efficient arm on Goal and Hard Goal, where some DLPA seeds never reach the threshold, and the most sample-efficient of the arms that act without a planner on all 7 tasks.

4.3. Ablations

We study the components on Goal and Hard Goal, the two sparse-success tasks on which most of the development took place (five seeds per cell). The cumulative ladder (Figure 5 and Table 4) adds them one at a time to the bare hybrid actor, in a fixed order; two final rows replace the hybrid actor with a relaxed continuous one, which yields the direct, naive adaptation of DreamerV3. The leave-one-out ablation (Table 5) removes one component from the full method.

Cumulative ladder. On Goal the bare agent fails on 3 of 5 seeds. SWR turns it into a learning agent (+0.43, interval +0.12 to +0.68); CME raises the score again (+0.09, interval +0.00 to +0.16) and shortens the *take-off*, the steps to the threshold, from 87.5k to 63.5k steps; ε-mode shortens it to 40k without raising the final score. On Hard Goal SWR makes every seed take off, but 2 of 5 then stall in a *parameter-saturation trap*: early in training a parameter mean saturates the $\tanh$, its gradient vanishes, and the success rate stays flat for the rest of the run. Adding CME brings every seed above 0.5, including seeds that enter the trap and later leave it. ε-mode re-opens the trap on 1 seed and μ-reg closes it. Along the ladder, SWR and CME account for most of the gain, ε-mode buys a faster take-off on Goal, and μ-reg is the guard ε-mode needs.

Relaxed actor. The direct adaptation of DreamerV3 keeps its continuous actor and gives it the relaxed action of PA-TD3 (Hausknecht & Stone, 2016): one vector with a score per mode and every mode's parameters, executed as the arg-max mode. We train this PA-Dreamer with everything else unchanged, with and without SWR. On Hard Goal it

Task	Budget	HyLI (ours)	DLPA†	HyAR	P-DQN‡	HHQN	PA-TD3	H-PPO
Platform	2e5	**1.00 ± 0.00**	0.97 ± 0.03	0.98 ± 0.01	0.84 ± 0.13	0.42 ± 0.22	0.92 ± 0.03	0.81 ± 0.03
Goal	3e5	**0.77 ± 0.03**	0.58 ± 0.29	0.74 ± 0.02	0.61 ± 0.20	0.00 ± 0.00	0.00 ± 0.00	0.00 ± 0.00
Hard Goal	3e5	**0.79 ± 0.04**	0.34 ± 0.28	0.59 ± 0.08	0.07 ± 0.08	0.02 ± 0.04	0.14 ± 0.18	0.00 ± 0.00
Catch Point	5e5	**0.94 ± 0.00**	0.92 ± 0.03	0.70 ± 0.18	0.92 ± 0.05	0.33 ± 0.17	0.59 ± 0.17	0.72 ± 0.06
Hard Move (n=4)	5e5	0.91 ± 0.05	0.94 ± 0.01	**0.95 ± 0.01**	0.30 ± 0.05	0.55 ± 0.19	0.49 ± 0.18	0.64 ± 0.12
Hard Move (n=6)	5e5	**0.95 ± 0.03**	*0.94 ± 0.01*	*0.93 ± 0.04*	0.34 ± 0.06	0.17 ± 0.05	0.07 ± 0.04	0.59 ± 0.19
Hard Move (n=8)	5e5	0.91 ± 0.06	**0.93 ± 0.01**	0.89 ± 0.06	0.14 ± 0.05	0.05 ± 0.04	0.08 ± 0.03	0.14 ± 0.05

Table 1. Final score on a common window: every arm is scored on its first B environment interactions (B: Budget column), mean ± std over 5 seeds of the mean of the final five evaluations (return on Platform, success rate elsewhere). †At its converged, shorter budget. ‡With a hand-coded parameter prior. Bold: best mean; italic: mean at least the best mean minus the best arm's standard deviation, both computed before rounding. Std: population standard deviation over seeds, as in Li et al. (2022). Full budgets and learning curves: Appendix F.

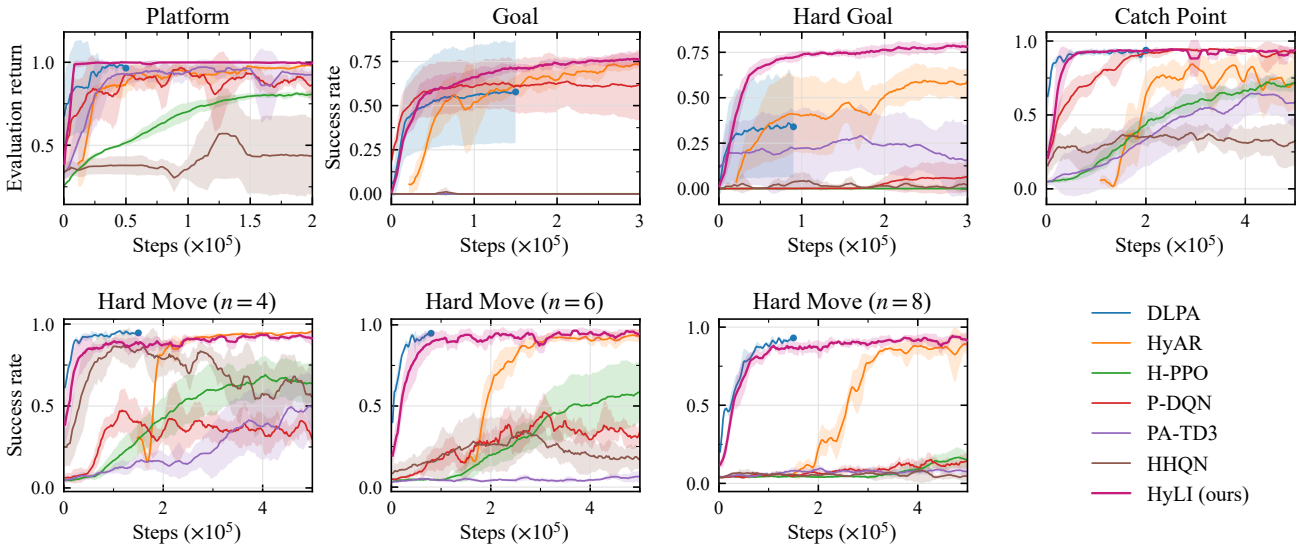


Figure 4. Learning curves in the metric of Table 1: evaluation success rate (return on Platform), mean ± std over 5 seeds. Each panel ends at our budget; arms with longer budgets are drawn up to it, and a dot marks the end of a shorter one (DLPA). Every interaction is on the step axis, HyAR's reward-free pre-training included; its curve therefore starts later. Episode return: Figure 11.

Task	K	HyLI (ours)	DLPA	HyAR	P-DQN	ratio
Platform	3	1.29	108	0.343	0.11	84×
Goal	3	1.3	51.6	0.347	0.112	40×
H. Goal	11	1.56	62	0.347	0.107	40×
Catch	2	1.28	52.4	0.337	0.106	41×
HM4	16	1.09	46.2	0.345	0.106	42×
HM6	64	1.1	95.9	0.346	0.109	87×
HM8	256	1.13	323	0.357	0.124	286×
HM10	1024	1.29	1145	0.381	0.222	888×

Table 2. Milliseconds per decision on one CPU thread, batch size 1, median of 1 000 decisions: for HyLI the encoder, recurrent step and actor; for DLPA a full MPPI plan. Same machine for all arms; GPU and all baselines in Appendix F. Ratio: DLPA over ours.

fails on every seed either way, −0.32 against the hybrid actor with SWR (interval −0.58 to −0.09). On Goal neither actor learns reliably without SWR. Adding SWR raises the hybrid actor from 0.24 to 0.67 (+0.43) but PA-Dreamer only from 0.49 to 0.57 (+0.08), so with SWR PA-Dreamer ends below the hybrid actor (−0.10, Table 4). PA-Dreamer fails by plateaus in the mode choice—shooting from the start or dribbling without shooting—not by saturation.

Leave-one-out. No single removal lowers the final score as much as the ladder steps do (Table 5), because the components overlap, as the ladder shows. The effect of a removal shows in the worst seed and the take-off: without ε-mode one Goal seed fails, without μ-reg one Hard Goal seed stays in the saturation trap, without SWR Hard Goal takes off later, and without CME the worst seed drops on both tasks.

4.4. Parameter-head isolation

Figure 6 compares the per-mode `sub` head with a shared `multi` head and with a `multi` head widened to the parameter count of `sub`. On Hard Goal the shared head reaches the score of `sub`, although its measured cross-mode interference stays clearly above zero. On Goal it is slightly lower only when its capacity is not matched, and the widened head

Task	HyLI (ours)	DLPA†	HyAR	HyAR§	P-DQN‡	HHQN	PA-TD3	H-PPO
Platform (0.88)	4.5k	**1.5k**	25k	14k	9k	>200k (2/5)	21.5k	>200k (0/5)
Goal (0.70)	**45k**	47k (4/5)	85.8k	65k	31.5k (4/5)	>300k (0/5)	>300k (0/5)	>300k (0/5)
Hard Goal (0.54)	**29.5k**	29k (3/5)	105k	84.5k	>300k (0/5)	>300k (0/5)	>300k (2/5)	>300k (0/5)
Catch Point (0.81)	20k	**10k**	221k	115k	105k	>500k (0/5)	>500k (2/5)	432k (4/5)
Hard Move (n=4) (0.84)	27.5k	**15k**	185k	40k	>500k (2/5)	55k	>500k (1/5)	>500k (2/5)
Hard Move (n=6) (0.83)	35k	**22.5k**	212k	67.5k	340k (4/5)	>500k (0/5)	>500k (0/5)	>500k (0/5)
Hard Move (n=8) (0.80)	62.5k	**47.5k**	275k	130k	>500k (0/5)	>500k (0/5)	>500k (0/5)	>500k (0/5)

Table 3. Environment steps to reach 90% of HyAR's published score (threshold in brackets), median over 5 seeds; (reached/5) when not every seed reaches it; >: censored at the arm's budget. Bold: fewest steps among the arms whose five seeds all reach the threshold, so that a fast median over partly failed seeds is not ranked first. HyAR's steps include its reward-free pre-training; §: HyAR without it (not ranked).

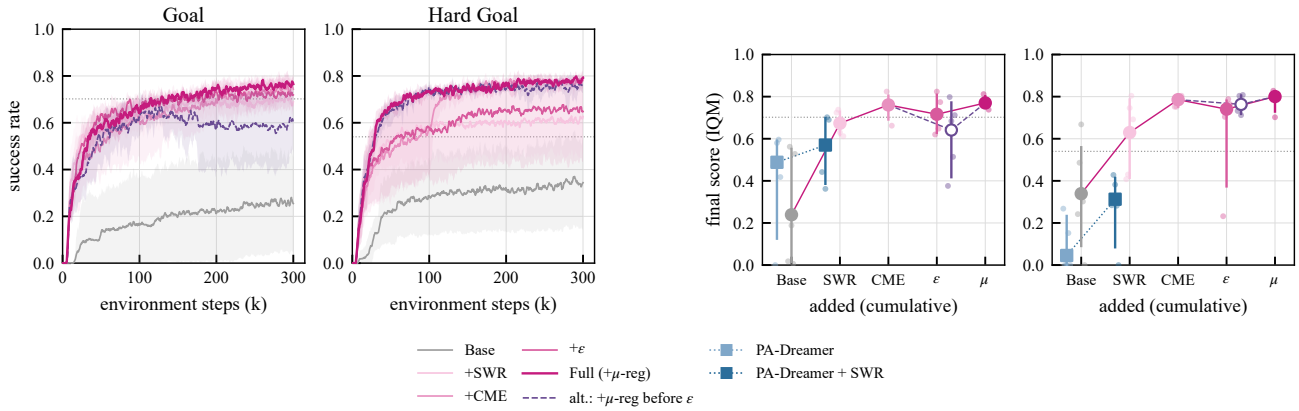


Figure 5. Cumulative ladder. Left: evaluation success rate, mean over 5 seeds with a 95% pointwise bootstrap band; dotted: 90% of HyAR's published score. Right: inter-quartile mean of the final score with its 95% bootstrap interval and the individual seeds after each component is added; hollow marker: the alternative path (+μ-reg before ε-mode); squares: PA-Dreamer without and with SWR. Each pair shows Goal on the left and Hard Goal on the right.

	Goal			Hard Goal		
	score	Δ	steps	score	Δ	steps
Base (all off)	0.24 (0.01) [3]	–	>300k (1/5)	0.34 (0.00) [4]	–	>300k (2/5)
+SWR	0.67 (0.61) [0]	+0.43 [+0.12, +0.68]	87.5k	0.63 (0.41) [2]	+0.29 [−0.04, +0.58]	34.5k
+CME	0.76 (0.66) [0]	+0.09 [+0.00, +0.16]	63.5k	0.79 (0.75) [0]	+0.16 [−0.00, +0.37]	30k
+ε-mode	0.72 (0.62) [0]	−0.04 [−0.14, +0.06]	40k	0.74 (0.23) [1]	−0.05 [−0.41, +0.01]	24k (4/5)
+μ-reg (full method)	0.77 (0.74) [0]	+0.05 [−0.03, +0.14]	45k	0.80 (0.70) [0]	+0.06 [−0.02, +0.42]	29.5k
alt.: +μ-reg before ε-mode	0.64 (0.38) [1]	−0.12 [−0.34, +0.01]	55.5k	0.76 (0.71) [0]	−0.02 [−0.07, +0.04]	24k
PA-Dreamer (relaxed actor)	0.49 (0.00) [3]	+0.25 [−0.24, +0.52]	>300k (1/5)	0.05 (0.00) [5]	−0.29 [−0.56, +0.01]	>300k (1/5)
+SWR	0.57 (0.36) [2]	−0.10 [−0.29, +0.05]	161k (3/5)	0.31 (0.00) [5]	−0.32 [−0.58, −0.09]	187.5k (3/5)

Table 4. Cumulative ladder, 5 seeds per row: inter-quartile mean of the final score (worst seed) [seeds below 0.5]; Δ: change against the row above with 95% bootstrap interval (alternative path: against +CME; PA-Dreamer: against the hybrid row with the same components, i.e. the effect of the actor; computed before rounding); steps: median steps to 90% of HyAR's published score. The last ladder row is the main-comparison cell.

closes the gap. On Hard Move (n=4) both heads reach the same score. Interference between heterogeneous parameters is therefore present but does not reduce performance on these tasks; we attribute none of our results to isolation, and the default head is within noise of its alternatives.

5. Related work

Model-free PAMDP methods. Masson et al. (2016) alternate between the discrete and the parameter policy; PA-DDPG (Hausknecht & Stone, 2016), built on DDPG (Lillicrap et al., 2016), and its TD3 variant PA-TD3 (Li et al., 2022) relax the hybrid action into one continuous vector; P-DQN and MP-DQN (Xiong et al., 2018; Bester et al., 2019)

	Goal		Hard Goal	
	score	steps	score	steps
Full method	0.77 (0.74) [0]	45k	0.80 (0.70) [0]	29.5k
−SWR	0.76 (0.69) [0]	47.5k	0.80 (0.75) [0]	42.5k
−CME	0.73 (0.63) [0]	46k	0.76 (0.62) [0]	23k
−μ-reg	0.72 (0.62) [0]	40k	0.74 (0.23) [1]	24k (4/5)
−ε-mode	0.64 (0.38) [1]	55.5k	0.76 (0.71) [0]	24k

Table 5. Leave-one-out: inter-quartile mean of the final score (worst seed) [seeds below 0.5], and median steps to 90% of HyAR's published score. 5 seeds per row. Curves: Appendix F.9.

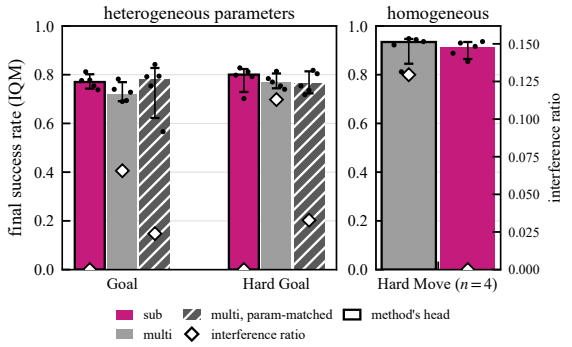


Figure 6. Parameter heads. Bars: inter-quartile mean of the final score, 95% bootstrap interval, 5 seeds (dots); black outline: the head the method uses. Diamonds (right axis): cross-mode interference ratio (zero for `sub`; Appendix A.3). Matched: `multi` widened to the parameter count of `sub`. Scores: Table 21.

output all modes' parameters and value each mode with a Q-function; HHQN (Fu et al., 2019) chooses the mode and then its parameters with two hierarchical networks; H-PPO (Fan et al., 2019), built on PPO (Schulman et al., 2017), and Hybrid SAC (Delalleau et al., 2019) use separate discrete and continuous actors; HyAR (Li et al., 2022) runs TD3 in a learned latent action space and defines the benchmark protocol we use; DA-AC (He et al., 2026) treats distribution parameters as actions. All act with a single forward pass of their networks; none uses a model.

Model-based PAMDP methods and decision-time computation. DLPA (Zhang et al., 2024) and FLEXplore (Wang et al., 2025) plan with MPPI in a learned model at every decision. DLPA also reports that a Dyna-like variant, which learns a policy from model rollouts, falls behind planning on Platform and Goal, so we compare against DLPA with planning, the stronger of the two; our ablations (Section 4.3) show which failures such a policy meets in a PAMDP and which components remove them. CHDP (Liu et al., 2026) runs a discrete and a continuous diffusion policy per decision, and KGRL (Ehrhardt et al., 2026) prunes actions with hand-written rules and refines parameters by gradient ascent on its Q-function at decision time. Closest to our approach, RAPS (Dalal et al., 2021) trains a Dreamer agent over robot manipulation primitives with a categorical primitive choice and one vector of all primitives' arguments, both trained with the score-function estimator; it is evaluated on manipulation suites, not on the PAMDP benchmarks, and is not compared with planners. HyLI differs in its separate estimator for each half of the action and in CME.

Evaluating every action. The expected policy gradient (Ciosek & Whiteson, 2018), mean actor-critic (Asadi et al., 2017) and many-actions policy gradients (Nauman & Cygan, 2023) integrate over several actions per state, the last also with a model; COMA (Foerster et al., 2018) uses a counterfactual baseline over one agent's actions; MuZero and Sampled MuZero (Schrittwieser et al., 2020; Hubert et al., 2021) evaluate candidates in a learned model at decision time. CME combines one model step per candidate mode with these estimators at training time only, so that it costs nothing when acting. TD-MPC2 (Hansen et al., 2024) plans in continuous action spaces only.

6. Limitations

Our ablations cover Goal and Hard Goal only, the tasks on which most of the development took place; of the trained tasks only Hard Move (n=8) was held out from development. Among the arms whose seeds all reach the threshold, DLPA still needs the fewest interactions on 5 of the 7 tasks, so the sample efficiency of learning a policy in imagination leaves room for improvement; a seed of HyLI also trains for tens of hours (Appendix G). The benchmark's episodes are short (a trained HyLI takes 3–6 decisions per episode on Goal and Hard Goal), which limits what the recurrent state can be credited for, and CME evaluates a capped candidate set, a biased approximation for large K; we train up to K=256. No code is available for CHDP or FLEXplore; we report CHDP's published results (Appendix C) and run neither.

7. Conclusion

Model-based PAMDP methods learn from far fewer interactions than model-free ones but plan at every decision, which limits how fast they can act. HyLI learns a hybrid policy in a world model's latent imagination and acts with one forward pass. CME gives every candidate mode a learning signal at every imagined state, and SWR keeps rare successes in training. On seven benchmarks, HyLI keeps comparable or better final performance while combining model-based sample efficiency with a policy's decision speed: 2.4× fewer interactions than HyAR and decisions 40 to 286× faster than DLPA. Longer horizons, where a critic can look beyond a planner's, are the next test.

Impact Statement

This paper presents work whose goal is to advance the field of machine learning, specifically reinforcement learning for actions that combine a discrete choice with continuous parameters. Its practical consequence is that such policies can be learned with fewer interactions and executed fast enough for real-time control loops, as in robots, vehicles and aircraft. Our results are on simulated benchmarks; success rates on them say nothing about the safety of a learned controller on a physical system, which requires verification and runtime safeguards beyond the scope of this work. We see no other societal consequence that must be highlighted here.

References

Agarwal, R., Schwarzer, M., Castro, P. S., Courville, A., and Bellemare, M. G. Deep reinforcement learning at the edge of the statistical precipice. In *Advances in Neural Information Processing Systems*, 2021.

Asadi, K., Allen, C., Roderick, M., Mohamed, A.-r., Konidaris, G., and Littman, M. Mean actor critic. arXiv preprint arXiv:1709.00503, 2017.

Bengio, Y., Léonard, N., and Courville, A. Estimating or propagating gradients through stochastic neurons for conditional computation. arXiv preprint arXiv:1308.3432, 2013.

Bester, C. J., James, S. D., and Konidaris, G. D. Multi-pass Q-networks for deep reinforcement learning with parameterised action spaces. *arXiv preprint arXiv:1905.04388*, 2019.

Bøhn, E., Coates, E. M., Moe, S., and Johansen, T. A. Deep reinforcement learning attitude control of fixed-wing UAVs using proximal policy optimization. In *International Conference on Unmanned Aircraft Systems (ICUAS)*, 2019.

Chen, X., Wang, C., Zhou, Z., and Ross, K. W. Randomized ensembled double Q-learning: Learning fast without a model. In *International Conference on Learning Representations*, 2021.

Ciosek, K. and Whiteson, S. Expected policy gradients. In *AAAI Conference on Artificial Intelligence*, 2018.

Dalal, M., Pathak, D., and Salakhutdinov, R. Accelerating robotic reinforcement learning via parameterized action primitives. In *Advances in Neural Information Processing Systems*, volume 34, 2021.

Delalleau, O., Peter, M., Alonso, E., and Logut, A. Discrete and continuous action representation for practical RL in video games. arXiv preprint arXiv:1912.11077, 2019.

D'Oro, P., Schwarzer, M., Nikishin, E., Bacon, P.-L., Bellemare, M. G., and Courville, A. Sample-efficient reinforcement learning by breaking the replay ratio barrier. In *International Conference on Learning Representations*, 2023.

Ehrhardt, J., Heesch, R., and Niggemann, O. Knowledge- and gradient-guided reinforcement learning for parametrized action Markov decision processes. arXiv preprint arXiv:2607.12924, 2026.

Fan, Z., Su, R., Zhang, W., and Yu, Y. Hybrid actor-critic reinforcement learning in parameterized action space. In *International Joint Conference on Artificial Intelligence*, 2019.

Feng, S., Li, X., Ren, L., and Xu, S. Reinforcement learning with parameterized action space and sparse reward for UAV navigation. *Intelligence & Robotics*, 3(2):161–175, 2023.

Foerster, J., Farquhar, G., Afouras, T., Nardelli, N., and Whiteson, S. Counterfactual multi-agent policy gradients. In *AAAI Conference on Artificial Intelligence*, 2018.

Fu, H., Tang, H., Hao, J., Lei, Z., Chen, Y., and Fan, C. Deep multi-agent reinforcement learning with discrete-continuous hybrid action spaces. In *International Joint Conference on Artificial Intelligence*, 2019.

Fujimoto, S., van Hoof, H., and Meger, D. Addressing function approximation error in actor-critic methods. In *International Conference on Machine Learning*, 2018.

Hafner, D., Lillicrap, T., Fischer, I., Villegas, R., Ha, D., Lee, H., and Davidson, J. Learning latent dynamics for planning from pixels. In *International Conference on Machine Learning*, 2019.

Hafner, D., Lillicrap, T., Ba, J., and Norouzi, M. Dream to control: Learning behaviors by latent imagination. In *International Conference on Learning Representations*, 2020.

Hafner, D., Lillicrap, T., Norouzi, M., and Ba, J. Mastering Atari with discrete world models. In *International Conference on Learning Representations*, 2021.

Hafner, D., Pasukonis, J., Ba, J., and Lillicrap, T. Mastering diverse control tasks through world models. *Nature*, 640(8059):647–653, 2025. doi: 10.1038/s41586-025-08744-2.

Hansen, N., Su, H., and Wang, X. TD-MPC2: Scalable, robust world models for continuous control. In *International Conference on Learning Representations*, 2024.

Hausknecht, M. and Stone, P. Deep reinforcement learning in parameterized action space. In *International Conference on Learning Representations*, 2016.

He, J., Mahmood, A. R., and White, M. Distributions as actions: A unified framework for diverse action spaces. In *International Conference on Learning Representations*, 2026.

Hiraoka, T., Imagawa, T., Hashimoto, T., Onishi, T., and Tsuruoka, Y. Dropout Q-functions for doubly efficient reinforcement learning. In *International Conference on Learning Representations*, 2022.

Hubert, T., Schrittwieser, J., Antonoglou, I., Barekatain, M., Schmitt, S., and Silver, D. Learning and planning in complex action spaces. In *International Conference on Machine Learning*, 2021.

Hwangbo, J., Lee, J., Dosovitskiy, A., Bellicoso, D., Tsounis, V., Koltun, V., and Hutter, M. Learning agile and dynamic motor skills for legged robots. *Science Robotics*, 4(26):eaau5872, 2019.

Jang, E., Gu, S., and Poole, B. Categorical reparameterization with Gumbel-softmax. In *International Conference on Learning Representations*, 2017.

Li, B., Tang, H., Zheng, Y., Hao, J., Li, P., Wang, Z., Meng, Z., and Wang, L. HyAR: Addressing discrete-continuous action reinforcement learning via hybrid action representation. In *International Conference on Learning Representations*, 2022.

Lillicrap, T. P., Hunt, J. J., Pritzel, A., Heess, N., Erez, T., Tassa, Y., Silver, D., and Wierstra, D. Continuous control with deep reinforcement learning. In *International Conference on Learning Representations*, 2016.

Lin, Y., Liu, X., and Zheng, Z. Discretionary lane-change decision and control via parameterized soft actor-critic for hybrid action space. arXiv preprint arXiv:2402.15790, 2024.

Liu, B., He, J., Shi, H., Wang, E., Han, W., Hao, J., Wang, P., and Zhang, Z. CHDP: Cooperative hybrid diffusion policies for reinforcement learning in parameterized action space. In *Proceedings of the AAAI Conference on Artificial Intelligence*, volume 40, pp. 23640–23648, 2026. doi: 10.1609/aaai.v40i28.39537.

Lowe, R., Wu, Y., Tamar, A., Harb, J., Abbeel, P., and Mordatch, I. Multi-agent actor-critic for mixed cooperative-competitive environments. In *Advances in Neural Information Processing Systems*, 2017.

Masson, W., Ranchod, P., and Konidaris, G. Reinforcement learning with parameterized actions. In *AAAI Conference on Artificial Intelligence*, 2016.

Nasiriany, S., Liu, H., and Zhu, Y. Augmenting reinforcement learning with behavior primitives for diverse manipulation tasks. In *IEEE International Conference on Robotics and Automation (ICRA)*, 2022.

Nauman, M. and Cygan, M. On many-actions policy gradient. In *Proceedings of the 40th International Conference on Machine Learning*, volume 202 of *Proceedings of Machine Learning Research*, 2023.

Neunert, M., Abdolmaleki, A., Wulfmeier, M., Lampe, T., Springenberg, T., Hafner, R., Romano, F., Buchli, J., Heess, N., and Riedmiller, M. Continuous-discrete reinforcement learning for hybrid control in robotics. In *Proceedings of the Conference on Robot Learning*, volume 100 of *Proceedings of Machine Learning Research*, 2020.

Nikishin, E., Schwarzer, M., D'Oro, P., Bacon, P.-L., and Courville, A. The primacy bias in deep reinforcement learning. In *International Conference on Machine Learning*, 2022.

Oh, J., Guo, Y., Singh, S., and Lee, H. Self-imitation learning. In *International Conference on Machine Learning*, 2018.

Rudin, N., Hoeller, D., Reist, P., and Hutter, M. Learning to walk in minutes using massively parallel deep reinforcement learning. In *Proceedings of the 5th Conference on Robot Learning*, volume 164 of *Proceedings of Machine Learning Research*, 2022.

Schaul, T., Quan, J., Antonoglou, I., and Silver, D. Prioritized experience replay. In *International Conference on Learning Representations*, 2016.

Schrittwieser, J., Antonoglou, I., Hubert, T., Simonyan, K., Sifre, L., Schmitt, S., Guez, A., Lockhart, E., Hassabis, D., Graepel, T., Lillicrap, T., and Silver, D. Mastering Atari, Go, chess and shogi by planning with a learned model. *Nature*, 588:604–609, 2020.

Schulman, J., Wolski, F., Dhariwal, P., Radford, A., and Klimov, O. Proximal policy optimization algorithms. arXiv preprint arXiv:1707.06347, 2017.

Wang, Z., Wang, B., Shao, M., Dou, H., and Tao, B. Learn a flexible exploration model for parameterized action Markov decision processes. arXiv preprint arXiv:2501.02774, 2025.

Williams, G., Wagener, N., Goldfain, B., Drews, P., Rehg, J. M., Boots, B., and Theodorou, E. A. Information theoretic MPC for model-based reinforcement learning. In *IEEE International Conference on Robotics and Automation (ICRA)*, 2017.

Wurman, P. R., Barrett, S., Kawamoto, K., MacGlashan, J., Subramanian, K., Walsh, T. J., Capobianco, R., Devlic, A., Eckert, F., Fuchs, F., Gilpin, L., Khandelwal, P., Kompella, V., Lin, H., MacAlpine, P., Oller, D., Seno, T., Sherstan, C., Thomure, M. D., Aghabozorgi, H., Barrett, L., Douglas, R., Whitehead, D., Dürr, P., Stone, P., Spranger, M., and Kitano, H. Outracing champion Gran Turismo drivers with deep reinforcement learning. *Nature*, 602:223–228, 2022.

Xiong, J., Wang, Q., Yang, Z., Sun, P., Han, L., Zheng, Y., Fu, H., Zhang, T., Liu, J., and Liu, H. Parametrized deep Q-networks learning: Reinforcement learning with discrete-continuous hybrid action space. *arXiv preprint arXiv:1810.06394*, 2018.

Zhang, R., Fu, H., Miao, Y., and Konidaris, G. Model-based reinforcement learning for parameterized action spaces. In *Proceedings of the 41st International Conference on Machine Learning*, volume 235 of *Proceedings of Machine Learning Research*, pp. 58935–58954, 2024.

A. Protocol and method details

Evaluation. Every arm is evaluated with the reference cadence (every 500 steps on Platform, Goal, Hard Goal; every 2 500 on the MPE tasks), 100 greedy episodes per evaluation, in a separate environment under a preserved random stream, so that evaluation never perturbs training. A run's score is the mean of its final five evaluations; cells report mean $\pm$ std over seeds 0–4. Because a single late evaluation dip can move this score, Appendix F repeats every cell with the mean over the last $\min(5 \cdot 10^4,\ 25\%$ of the budget) steps. Curves plot the per-task metric of the tables; Figure 11 repeats Figure 4 in episode return, the quantity the reference papers plot. Hard Move (n=10) is not trained, to keep the compute budget (its 1024 nominal modes collapse to 211 distinct motions, Appendix D.3); it appears in the latency table and, with its published numbers, in Appendix C.

Budgets and interaction accounting. Every environment interaction counts, warm-up included (Table 14); HyAR's reward-free pre-training episodes are added to its step axis. HyLI runs $\min(\text{reference}, 5{\times}10^5)$ steps per task (Table 12); the model-free arms run the reference budgets. All arms are scored on their first B environment interactions, with B our budget on the task, pre-training included: an arm that ran longer is cut at B and its final five evaluations within the window are its score. Scoring each arm at its own, longer budget would not be neutral: several baselines decline late in training (HyAR on Hard Move (n=4), for instance), so a longer budget can lower their score; those scores are in Table 15. DLPA's planner makes the reference budgets impractical (its decision cost is paid at every training step), so it runs to its *converged* budget: the budget of Zhang et al. (2024, Fig. 4) or, where it is not within one published standard deviation of its published return there, until it converges, capped at ours (Table 11). Its cells are never compared at a budget it did not run.

Baselines and tuning. P-DQN, PA-TD3, HHQN, H-PPO and HyAR run from the reference code with its per-task settings, verified file by file; for HyAR, P-DQN and HHQN we run the TD3 variants, whose published numbers are the strongest. DLPA is ported from its official code and verified bit-exact against it (Appendix E). CHDP has no released code and appears only as published numbers. Every baseline runs with the per-task settings its authors published for these tasks, without re-tuning; while adding our own components we tried variants on every trained task except Hard Move (n=8), mostly on Goal and Hard Goal, then fixed one configuration; Hard Move (n=8) was not used to choose any component or setting. Our own settings are reduced from the DreamerV3 defaults for environment scale and budget and are the same on every task except where Appendix E.1 states otherwise. Our replay ratio (256 replayed steps per environment step, Table 6) is also higher than the model-free baselines' defaults. Raising the replay ratio of model-free agents is known to require additional stabilization (ensembles, regularization or resets; Chen et al., 2021; Hiraoka et al., 2022; Nikishin et al., 2022; D'Oro et al., 2023), and building such a variant of HyAR is outside the scope of this work. The model-based baseline DLPA already performs more updates per environment step than HyLI (25 updates of batch 64 after every step).

Sample efficiency and statistics. A fixed, external threshold (90% of HyAR's published score) is defined for every arm, including DLPA at its shorter budget; the area under the curve is not, and appears only over our own budget (Appendix F), which also repeats the analysis at 75% and 100%. For ablations we report the inter-quartile mean with 95% bootstrap intervals (Agarwal et al., 2021) together with the worst seed and the number of failing seeds, because at five seeds the tail is more informative than a difference in means.

A.1. Action representation

The world model receives the hybrid action as $[\,\text{onehot}(k) \mid x_1 \mid \ldots \mid x_K\,]$ with every slice except the selected mode's set to zero (*blocked* layout). Each parameter slot belongs to exactly one mode and no two modes alias the same input unit, which matters when parameter semantics are heterogeneous. When they are homogeneous a *padded* layout $[\,\text{onehot}(k) \mid x_k\,]$ is equivalent and smaller; we use it on Hard Move. The layout is set independently of the actor's parameter head.

A.2. Training details

Replay samples windows of $16{\times}32$ steps with one update every two environment steps; windows may cross episode boundaries, where the RSSM state is reset, and truncation is not written as termination. Imagination starts from every posterior state of the batch, with step weights $\prod_{t'<t} \gamma \hat{c}_{t'}$, where $\hat{c}_0$ is 0 if the *real* start state is terminal and 1 otherwise: on tasks whose episodes often end after one or two decisions (Goal and Hard Goal early in training), a randomly drawn start is often terminal, and without this weight much of the actor-critic signal would be built on imagined continuations of finished episodes. The return scale S of Section 3.3 is DreamerV3's: $\max(1, P_{95} - P_5)$ of the λ-returns, with both percentiles

averaged at decay 0.99; the actor loss uses the same scale. CME subtracts the stop-gradient baseline $b = \sum_j \pi_j V_j$ from both of its terms, which changes neither gradient. The continuous entropy uses the pre-squash Gaussian as a proxy for the squashed distribution. SWR uses each task's own success rule and is off on Platform, which has no sparse success event. ε-mode exploration changes only the acting policy; imagination, the losses and evaluation are unchanged. The random prefill follows one rule: where a random policy succeeds in fewer than one episode in a thousand (Goal, Hard Goal) we prefill $5\,000$ steps and use ε-mode exploration; elsewhere we prefill $1\,000$ steps without it. Prefill counts against the budget.

A.3. Interference without harm

We measure interference directly: an update driven by one mode's parameters is applied to the actor, and the resulting change in the other modes' parameters is divided by the change in its own (the *interference ratio*; zero by construction for `sub`). The measurement confirms that a shared head transfers updates across modes on the heterogeneous tasks, but not that this costs score (Section 4.4). A plausible reading is that CME, which trains every candidate's parameters toward its own value, supplies each mode with a signal strong enough to absorb the disturbance.

B. Reproducibility

Settings. Table 6 lists our settings against the DreamerV3 defaults, with the reason for each change. The same configuration is used for every experiment reported here; the defaults block of our configuration has every component switched off, so every ablation row is the task's configuration with switches set back: a leave-one-out row switches off one component of the full method, and the ladder rows switch the components on one at a time, in a fixed order, from the base with all of them off. Baselines use the settings of the reference code (Appendix E). Seeds are 0–4 for every arm, the seed loop of the reference drivers. Our agent is a PyTorch re-implementation that follows the official JAX code of DreamerV3; every difference we know of is listed in Table 6, and we did not test numerical equivalence with the official code. It mixes two DreamerV3 versions in two places, both stated in Table 6: a pathwise parameter gradient as in the 2023 preprint (arXiv:2301.04104v1), with the critic's bootstrap values detached in the λ-return term (the current version uses REINFORCE for every action; CME's parameter term needs a pathwise path, and it does differentiate through the critic, whose weights it does not update), and the output scale 0.01 of the current version.

Setting	DreamerV3	Ours (reason)
deterministic state	512	256 (4–17-dim observations)
stochastic state	32×32	16×16 (same)
MLP width / embed	512 / 256	256 / 128 (same)
imagination horizon	15	10 (short episodes)
discount γ	0.997	0.99 (short episodes)
model / actor / critic lr	1e-4 / 3e-5 / 3e-5	3e-4 / 1e-4 / 1e-4 (budgets $\leq 5 \cdot 10^5$)
optimizer	Adam, ϵ 1e-8 model / 1e-5 actor-critic (2023)	Adam, ϵ 1e-8
batch $\times$ length	16×64	16×32
replayed steps per env step	32 (32–1024 per domain)	256 (update every 2 steps)
imagination starts	all replayed states	all replayed states
parameter gradient	pathwise (2023) / REINFORCE (current)	pathwise, critic values detached
entropy coefficient	3e-4	3e-4, discrete and continuous, every task
output-layer scale	0.01 (current)	0.01; parameter head 1
parameter head	–	`multi` (Hard Move), `sub` elsewhere
world-model action layout	–	padded (Hard Move), blocked elsewhere
parameter mean bound	–	$5\tanh(\mu/5)$ (changes $\tanh\mu$ by < 0.01)
CME candidates	–	all if $K \leq 16$, else top-8 + 8 random
SWR fraction ρ	–	0.25 (off on Platform)
SWR success event	–	a goal (Goal, Hard Goal); reward > 4 (MPE)
μ-regularization	–	0.01, threshold $\lvert\mu\rvert = 3$, every task
ε-mode exploration	–	$0.1\to0$ over $5 \cdot 10^4$ steps (Goal, Hard Goal)
prefill	–	5 000 (Goal/Hard Goal), 1 000 elsewhere; counted

Table 6. Our settings, identical on every task except where a task is named.

Training cost of CME. Table 7 reports the time of one full update (world model, actor and critic) for the full method, for the base configuration of the ladder (CME, ε-mode and μ-reg off; SWR only changes which windows are sampled) and for

PA-Dreamer. The world-model part takes the same time in every variant. CME multiplies the update by about 1.4 with two or three candidates and by 2 to 2.6 with eleven to sixteen; with the candidate cap it grows little beyond $K{=}16$ (Hard Move ($n{=}8$)). PA-Dreamer's actor, with one output vector, is the cheapest. Decision time is unchanged by every training component.

Task	K	candidates	base	full method	ratio	PA-Dreamer
Goal	3	3	115	169	1.47×	103
Hard Goal	11	11	122	247	2.03×	100
Catch Point	2	2	116	159	1.37×	–
Hard Move ($n{=}4$)	16	16	112	262	2.34×	–
Hard Move ($n{=}8$)	256	16	111	284	2.56×	–

Table 7. Milliseconds per full update (batch 16×32), single process with nothing else running, one RTX A4000. Base: CME, ε-mode and μ-reg off. Ratio: full method over base. Measured on five of the seven tasks.

C. Published numbers

Table 8 quotes the TD3-based block and the H-PPO column of Li et al. (2022), which our model-free arms correspond to, including Hard Move ($n{=}10$), which we do not train (Appendix A). Table 9 quotes DLPA's published episode returns (our tables report the success rate, Table 1; our DLPA runs in that metric: Table 11) and CHDP's published results, which we cannot reproduce because no code is available; we make no claim of superiority over CHDP.

Task	H-PPO	PA-TD3	P-DQN-TD3	HHQN-TD3	HyAR-TD3
Platform	0.80 ± 0.02	0.94 ± 0.10	0.93 ± 0.03	0.62 ± 0.23	0.98 ± 0.01
Goal	0.00 ± 0.00	0.00 ± 0.00	0.71 ± 0.07	0.00 ± 0.00	0.78 ± 0.03
Hard Goal	0.00 ± 0.00	0.44 ± 0.05	0.06 ± 0.07	0.01 ± 0.01	0.60 ± 0.07
Catch Point	0.69 ± 0.09	0.82 ± 0.10	0.89 ± 0.07	0.27 ± 0.05	0.90 ± 0.03
Hard Move ($n{=}4$)	0.09 ± 0.02	0.66 ± 0.13	0.85 ± 0.10	0.52 ± 0.17	0.93 ± 0.02
Hard Move ($n{=}6$)	0.05 ± 0.01	0.04 ± 0.02	0.74 ± 0.08	0.29 ± 0.13	0.92 ± 0.04
Hard Move ($n{=}8$)	0.04 ± 0.01	0.06 ± 0.02	0.05 ± 0.02	0.05 ± 0.02	0.89 ± 0.03
Hard Move ($n{=}10$)	0.05 ± 0.01	0.07 ± 0.02	0.05 ± 0.02	0.05 ± 0.02	0.75 ± 0.05

Table 8. Published success rates (return on Platform), Li et al. (2022), Table 2, TD3-based methods.

	Platform	Goal	Hard Goal	Catch Point	HM4	HM6	HM8	HM10
DLPA (published)	0.92 ± 0.05	28.75 ± 6.91	28.38 ± 2.88	7.56 ± 4.86	6.29 ± 5.74	8.48 ± 5.45	7.80 ± 6.27	6.35 ± 9.97
CHDP (published)	99.7 ± 0.2	80.9 ± 4.9	79.5 ± 5.0	93.8 ± 0.6	94.2 ± 1.7	93.9 ± 1.0	90.6 ± 2.2	79.8 ± 5.4

Table 9. DLPA: published episode return (mean of the last 10 evaluations), Table 1 of Zhang et al. (2024). CHDP: success rate in percent, mean $\pm$ std over 5 runs, each the mean of its final five evaluations, Table 1 of Liu et al. (2026).

Reproduction quality. Table 10 compares every model-free arm we ran with its published TD3-block result, at the arm's own budget (the setting of the published numbers) and on the common window of Table 1. Of 35 comparable cells, 24 lie within two published standard deviations; 7 lie below and 4 above, so the deviations do not favor our method systematically: the largest ones are in favor of a baseline (H-PPO on Hard Move). For P-DQN on Platform and PA-TD3 on Catch Point, the released code run in our environments does not reach the published result; the other cells below -2σ are discussed next.

HyAR on Hard Move ($n{=}4$)/Hard Move ($n{=}8$). On the common window our runs match the published values; they fall below only at the full 10^6 budget, where the success rate declines late in training (Figure 9). Li et al. (2022) do not define which end-of-training statistic their Table 2 reports (last evaluation, an average of the last few, or the best one), so a late decline is invisible in the published number under some of these definitions. We report the final-5 mean for every arm.

PA-TD3 and HHQN on Hard Goal. The reference Hard Goal drivers of these two arms, unlike their drivers for the other tasks, anneal the exploration-noise standard deviation linearly from 1.0 to 0.1 over the first 1000 episodes; our port does the same. With the annealing, HHQN reproduces its published value. PA-TD3 stays below it: four of five seeds learn (best

evaluation between 0.38 and 0.67), and three of them later return to the shoot-at-once optimum. The remaining known difference is the episode cap: the published Goal/Hard Goal values of both arms were obtained with 250 steps, where we use 150 for every arm (Appendix E).

DA-AC. He et al. (2026) report hybrid-action results on the same suite against PA-TD3, P-DQN and HHQN only. At its reported budgets its learning curves stay below HyAR's published TD3 scores on Platform, Goal, Hard Goal, Hard Move (n=6) and Hard Move (n=8), and above them on Catch Point and Hard Move (n=4), where it may be a stronger model-free baseline than HyAR. We do not run it.

P-DQN on Hard Move (n=4)/Hard Move (n=6). The audit found no difference from the reference driver: arguments, Ornstein–Uhlenbeck noise, ϵ schedule and evaluation all match.

Arm	Task	published	ours, own budget	ours, common window	$\Delta/\sigma_{\text{pub}}$
HyAR	Platform	0.98 ± 0.01	0.97 ± 0.03	0.98 ± 0.01	-0.8
	Goal	0.78 ± 0.03	0.74 ± 0.03	0.74 ± 0.02	-1.3
	Hard Goal	0.60 ± 0.07	0.57 ± 0.11	0.59 ± 0.08	-0.4
	Catch Point	0.90 ± 0.03	0.85 ± 0.15	0.70 ± 0.18	-1.7
	Hard Move (n=4)	0.93 ± 0.02	0.84 ± 0.09	0.95 ± 0.01	$\mathbf{-4.6}$
	Hard Move (n=6)	0.92 ± 0.04	0.87 ± 0.06	0.93 ± 0.04	-1.2
	Hard Move (n=8)	0.89 ± 0.03	0.81 ± 0.13	0.89 ± 0.06	$\mathbf{-2.7}$
P-DQN	Platform	0.93 ± 0.03	0.84 ± 0.13	0.84 ± 0.13	$\mathbf{-2.9}$
	Goal	0.71 ± 0.07	0.61 ± 0.20	0.61 ± 0.20	-1.4
	Hard Goal	0.06 ± 0.07	0.07 ± 0.08	0.07 ± 0.08	$+0.1$
	Catch Point	0.89 ± 0.07	0.92 ± 0.03	0.92 ± 0.05	$+0.4$
	Hard Move (n=4)	0.85 ± 0.10	0.43 ± 0.07	0.30 ± 0.05	$\mathbf{-4.2}$
	Hard Move (n=6)	0.74 ± 0.08	0.33 ± 0.09	0.34 ± 0.06	$\mathbf{-5.2}$
	Hard Move (n=8)	0.05 ± 0.02	0.14 ± 0.07	0.14 ± 0.05	$\mathbf{+4.7}$
HHQN	Platform	0.62 ± 0.23	0.42 ± 0.22	0.42 ± 0.22	-0.9
	Goal	0.00 ± 0.00	0.00 ± 0.00	0.00 ± 0.00	$+0.0$
	Hard Goal	0.01 ± 0.01	0.02 ± 0.04	0.02 ± 0.04	$+1.0$
	Catch Point	0.27 ± 0.05	0.24 ± 0.14	0.33 ± 0.17	-0.7
	Hard Move (n=4)	0.52 ± 0.17	0.36 ± 0.19	0.55 ± 0.19	-0.9
	Hard Move (n=6)	0.29 ± 0.13	0.29 ± 0.17	0.17 ± 0.05	$+0.0$
	Hard Move (n=8)	0.05 ± 0.02	0.04 ± 0.02	0.05 ± 0.04	-0.4
PA-TD3	Platform	0.94 ± 0.10	0.92 ± 0.03	0.92 ± 0.03	-0.2
	Goal	0.00 ± 0.00	0.00 ± 0.00	0.00 ± 0.00	$+0.0$
	Hard Goal	0.44 ± 0.05	0.14 ± 0.18	0.14 ± 0.18	$\mathbf{-5.9}$
	Catch Point	0.82 ± 0.10	0.50 ± 0.05	0.59 ± 0.17	$\mathbf{-3.2}$
	Hard Move (n=4)	0.66 ± 0.13	0.85 ± 0.07	0.49 ± 0.18	$+1.4$
	Hard Move (n=6)	0.04 ± 0.02	0.04 ± 0.02	0.07 ± 0.04	-0.2
	Hard Move (n=8)	0.06 ± 0.02	0.08 ± 0.03	0.08 ± 0.03	$+1.1$
H-PPO	Platform	0.80 ± 0.02	0.81 ± 0.03	0.81 ± 0.03	$+0.5$
	Goal	0.00 ± 0.00	0.00 ± 0.00	0.00 ± 0.00	$+0.1$
	Hard Goal	0.00 ± 0.00	0.00 ± 0.00	0.00 ± 0.00	$+0.0$
	Catch Point	0.69 ± 0.09	0.76 ± 0.06	0.72 ± 0.06	$+0.8$
	Hard Move (n=4)	0.09 ± 0.02	0.64 ± 0.07	0.64 ± 0.12	$\mathbf{+27.6}$
	Hard Move (n=6)	0.05 ± 0.01	0.63 ± 0.10	0.59 ± 0.19	$\mathbf{+57.8}$
	Hard Move (n=8)	0.04 ± 0.01	0.52 ± 0.16	0.14 ± 0.05	$\mathbf{+47.6}$

Table 10. Reproduced against published success rates (return on Platform; Li et al. (2022), Table 2, TD3 block). Own budget: the arm's reference budget, as in the publication. Common window: Table 1. Last column: deviation of the own-budget mean in units of the published standard deviation (floor 0.01); bold beyond ± 2.

DLPA. Table 11 compares our DLPA runs with its published results in its own metric, the episode return averaged over the last 10 evaluations, under our protocol (Appendix E). At the budget of Zhang et al. (2024, Fig. 4), our runs are within one published standard deviation of the published return on Catch Point, Hard Move (n=4) and Hard Move (n=6), and below it by more on Platform, Goal, Hard Goal and Hard Move (n=8); by the budget rule (Appendix A) these four runs are extended until they converge. At the converged budget every task is within one published standard deviation or above, except Hard Goal: two of its five seeds stay at the shoot-at-once optimum (success rate 0) and are kept, as is the one such seed on Goal

(Appendix E).

		budget of Zhang et al. (2024, Fig. 4)			converged budget		
Task	published	steps	ours	z	steps	ours	z
Platform	0.92 ± 0.05	2e4	0.85 ± 0.28	-1.5	5e4	0.98 ± 0.02	$+1.1$
Goal	28.75 ± 6.91	2e4	16.54 ± 11.51	-1.8	1.5e5	25.99 ± 16.09	-0.4
Hard Goal	28.38 ± 2.88	5e4	11.66 ± 14.68	$\mathbf{-5.8}$	9e4	13.17 ± 15.82	$\mathbf{-5.3}$
Catch Point	7.56 ± 4.86	2e5	6.90 ± 0.64	-0.1		not extended	
Hard Move (n=4)	6.29 ± 5.74	1.5e5	6.91 ± 0.49	$+0.1$		not extended	
Hard Move (n=6)	8.48 ± 5.45	8e4	5.69 ± 0.80	-0.5		not extended	
Hard Move (n=8)	7.80 ± 6.27	2e4	-17.44 ± 1.83	$\mathbf{-4.0}$	1.5e5	5.43 ± 0.20	-0.4

Table 11. DLPA: published episode return (Zhang et al., 2024, Table 1) against our runs, per seed the mean of the last 10 evaluations, mean $\pm$ std over 5 seeds. z: deviation from the published mean in units of the published standard deviation; bold beyond ± 2. Converged budget: the budget of Table 1.

D. Environments

D.1. Tasks and protocol constants

						budget (env steps)			
Task	K	$\sum_k d_k$	eval every	max steps	metric	reference	ours	DLPA	DLPA (published)
Platform	3	3	500	250	return	2e5	2e5	5e4	2e4
Goal	3	4	500	150	success	3e5	3e5	1.5e5	2e4
Hard Goal	11	12	500	150	success	3e5	3e5	9e4	5e4
Catch Point	2	2	2 500	25	success	1e6	5e5	2e5	2e5
Hard Move (n=4)	16	16	2 500	30	success	1e6	5e5	1.5e5	1.5e5
Hard Move (n=6)	64	64	2 500	30	success	1e6	5e5	8e4	8e4
Hard Move (n=8)	256	256	2 500	30	success	1e6	5e5	1.5e5	2e4
Hard Move (n=10)	1024	1024	–	–	(latency only)	–	–	–	–

Table 12. Tasks and the protocol constants of the reference implementation. Last four columns: budgets in environment steps.

Success is defined as in the reference implementation: on Goal and Hard Goal an episode succeeds when its terminal step yields the goal reward of 50 (an episode that ends without a goal ends with the negative distance of the ball to the goal); on Catch Point and Hard Move when some step yields a reward above 4. Platform reports the normalized episode return.

D.2. Notes on two reference implementations

Catch Point parameters. The reference drivers give the two Catch Point modes one shared scalar parameter, the movement angle, which the catch mode does not use. Following the PAMDP definition, we give each mode its own parameter; our environment adapter maps it to the same executed action, and a golden-trace test against reference rollouts confirms that the environment is unchanged. The only difference is that every agent's parameter vector has two entries instead of one.

HHQN-TD3. The released implementation computes its second critic head through the first head's layers, so clipped double-Q is absent; it has no target policy smoothing and no delayed policy update, and it does not update its target parameter network. We ran the file unmodified, as published. These properties are consistent with its wide seed variance (published 0.62 ± 0.23 on Platform).

D.3. Degeneracy of Hard Move

Task	nominal modes	distinct motions	zero-motion modes
Hard Move (n=4)	16	9	4
Hard Move (n=6)	64	19	10
Hard Move (n=8)	256	81	16
Hard Move (n=10)	1024	211	34

Table 13. Opposing actuators cancel, so the nominal modes of Hard Move collapse to far fewer distinct motions.

Mode k of Hard Move applies the sum of the actuator directions encoded by the bits of k, so opposing actuators cancel: the 2^n nominal modes collapse to 9, 19, 81 and 211 distinct motions for $n = 4, 6, 8, 10$, of which 4, 10, 16 and 34 produce no motion at all. A learned policy leaves these modes: the share of dead modes it selects falls from its uniform value of 25%, 16% and 6% for $n = 4, 6, 8$ to 1.2%, 0.5% and 0.6% in the last tenth of training (mean over seeds). The released planner loops over the nominal modes serially (Appendix E), so its cost (Table 2) grows with their number, not with the number of distinct behaviors.

E. Baseline reproduction notes

Sources. P-DQN, PA-TD3, HHQN, H-PPO and HyAR: agent files vendored unchanged from the reference repository, driver logic ported, every per-task setting checked against the drivers' defaults. DLPA: ported from the official code and compared bit-exact on the CPU (weights, forward pass, losses and the optimizer step, planner, replay windows) against it.

HyAR's pre-training. HyAR trains its action representation on reward-free random episodes before its first update. These environment steps are not counted by the reference code; we add them to its step axis in every curve, in Table 3 and in Figure 3; Table 3 also reports its steps without them.

Warm-up and interaction accounting. Table 14 lists every arm's warm-up phase and whether it is counted.

Arm	Warm-up	Counted in budget
HyAR	pre-training: 5 000 random episodes (20 000 on Goal/Hard Goal) that train only the action VAE; then 128 random steps before the first policy update	yes, both (the reference code does not count the pre-training; we add it)
DLPA	first 50 episodes with random actions, no model update	yes
PA-TD3, HHQN	128 steps with the noisy (not random) policy, no update	yes
P-DQN	128 steps (500 on Platform), ϵ-greedy from ϵ=1, no update	yes
H-PPO	none (on-policy)	–
HyLI	random prefill: 5 000 steps on Goal/Hard Goal, 1 000 elsewhere; then ε-mode exploration (ε 0.1→0 over $5 \cdot 10^4$ steps) on Goal/Hard Goal only	yes

Table 14. Warm-up phases. Every counted interaction is on the x-axis of every figure; HyAR's pre-training is added to its axis.

Deviations from the reference code. (i) Evaluation runs in a separate environment under a preserved random stream; the reference evaluates inside the training loop, which changes the training environment's random state. (ii) One episode cap per task for every arm: 25 on Catch Point, where H-PPO's driver uses 30, and 150 on Goal and Hard Goal, the value of HyAR's drivers, where PA-TD3 and HHQN were published with 250. (iii) A Goal budget of $3 \cdot 10^5$ for every model-free arm, where H-PPO's driver uses $2 \cdot 10^5$. (iv) HyAR's zero-padding of unused parameter slots follows its Hard Goal driver on Goal as well, where its Goal loop omits it. (v) Catch Point gives each mode its own parameter (Appendix D.2); HyAR keeps the reference embedding sizes (4/4). (vi) Reference arguments that no driver reads (P-DQN's `multipass`, `split`, `action-input-layer`, `reward-scale`) are not reproduced, and where HyAR's paper and its drivers disagree (episode horizons in its Appendix B.1) we follow the drivers. All deviations will be documented with the code release.

Reference settings that are easy to miss. The following are reproduced from the reference drivers, not changed. P-DQN's hyperparameters differ per task (discount, warm-up, buffer size, target rates, learning rate and gradient clipping); its hand-coded passthrough initialization is active on Platform and Goal only. HyAR's replay buffers differ per task (10^6 transitions on Hard Move, 10^5 elsewhere; $2 \cdot 10^6$ for the embedding buffer on Goal and Hard Goal), and its target-policy noise is 0.1 where the PA-TD3 and HHQN drivers use 0.2. PA-TD3 and HHQN anneal their exploration noise from 1.0 to 0.1 over the first 1000 episodes on Hard Goal only; elsewhere it is a constant 0.1.

DLPA. (i) The released code augments the Catch Point observation with two history features (a failed-catch counter and a step counter) that the paper does not describe and no other method receives; we run without them, so all methods observe the same state. (ii) The released harness trains on 25-step episodes on every task and cuts the training episode at each evaluation; we use the protocol caps and do neither. (iii) Where the paper's and the code's hyperparameters differ we use the code's. (iv) Budgets: the budget of Zhang et al. (2024, Fig. 4); where our run is not within one published standard deviation of the published return there, it is extended until it converges, capped at our budget (Table 12); convergence is a last-quarter slope within evaluation noise. Table 11 compares both budgets with the published returns. (v) Hard Goal is not runnable from the released code (a missing padding function); our environment adapter provides it. (vi) Hard Move (n=8): at that budget our reproduction is well below the published return, and the official 25-step episode cap does not close the gap (two seeds), so the run is extended by the rule above (Table 12). At the extended budget it reaches the best mean of every arm on Hard Move (n=8) (Table 1). (vii) On Goal and Hard Goal some seeds lock into the shoot-at-once optimum (episode length 1, return -6.2) from the start; they are kept (no seed selection). Extending these seeds beyond the converged budget (to $3 \cdot 10^5$ steps on Goal and $1.6 \cdot 10^5$ on Hard Goal) does not free them, so a longer budget would not change DLPA's cells. (viii) Latency: the released planner loops over modes serially and synchronizes with the CPU at every decision; we keep this structure, which is why a GPU helps DLPA only at small K. On Platform, the slowest task at small K, the longest planning horizon of the suite (L=10, against 5 on Catch Point and Hard Move) dominates instead. (ix) We compare against the strongest published form of each approach, since our aim is an agent that stays at state-of-the-art final performance while being sample-efficient and fast at decision time. For model-based PAMDP methods this is DLPA with planning: Zhang et al. (2024, Sec. 6.2, Fig. 5a) evaluate a Dyna-style variant that trains a policy on model rollouts and report that it falls behind planning on Platform and Goal. A weaker variant that acts faster would add a point to the trade-off of Figure 3, not a stronger competitor; an arm that does not reach the threshold appears there only as a bound. A lower planner budget shortens DLPA's decision roughly in proportion to I (Hard Move (n=4), one CPU thread: 15.7 ms at I=2, 7.9 ms at I=1). By this scaling the released planner would act above 50 Hz at I=2 on some tasks (Hard Move (n=4)) but not on Platform or Hard Move (n=8), and at I=1 still not on Hard Move (n=8). Whether DLPA keeps its sample efficiency at such budgets is not tested here.

E.1. Our own settings

Every change from the DreamerV3 defaults is listed with its reason in Table 6. None was searched per task. The per-task choices follow fixed rules: the parameter head (`multi` where every mode has the same single parameter, Section 3.1), the world-model action layout (*padded* under the same condition, *blocked* otherwise, Appendix A.1), the SWR success event by each task's success rule (SWR off on Platform, which has no sparse success event), and ε-mode with a longer prefill where a random policy almost never succeeds (Appendix A.2).

F. Additional results

F.1. Scores at each arm's full budget

Table 15 scores every arm at its own budget instead of the common window of Table 1: HyLI at $\min(\text{reference}, 5 \cdot 10^5)$, the model-free arms at the reference budgets (up to 10^6 steps), DLPA at its converged budget.

Task	Budget	HyLI (ours)	DLPA†	HyAR	P-DQN‡	HHQN	PA-TD3	H-PPO
Platform	2e5	**1.00 ± 0.00**	0.97 ± 0.03	0.97 ± 0.03	0.84 ± 0.13	0.42 ± 0.22	0.92 ± 0.03	0.81 ± 0.03
Goal	3e5	**0.77 ± 0.03**	0.58 ± 0.29	0.74 ± 0.03	0.61 ± 0.20	0.00 ± 0.00	0.00 ± 0.00	0.00 ± 0.00
Hard Goal	3e5	**0.79 ± 0.04**	0.34 ± 0.28	0.57 ± 0.11	0.07 ± 0.08	0.02 ± 0.04	0.14 ± 0.18	0.00 ± 0.00
Catch Point	5e5 / 1e6	**0.94 ± 0.00**	0.92 ± 0.03	0.85 ± 0.15	0.92 ± 0.03	0.24 ± 0.14	0.50 ± 0.05	0.76 ± 0.06
Hard Move (n=4)	5e5 / 1e6	0.91 ± 0.05	**0.94 ± 0.01**	0.84 ± 0.09	0.43 ± 0.07	0.36 ± 0.19	0.85 ± 0.07	0.64 ± 0.07
Hard Move (n=6)	5e5 / 1e6	**0.95 ± 0.03**	*0.94 ± 0.01*	0.87 ± 0.06	0.33 ± 0.09	0.29 ± 0.17	0.04 ± 0.02	0.63 ± 0.10
Hard Move (n=8)	5e5 / 1e6	0.91 ± 0.06	**0.93 ± 0.01**	0.81 ± 0.13	0.14 ± 0.07	0.04 ± 0.02	0.08 ± 0.03	0.52 ± 0.16

Table 15. Final performance with every arm scored at its own budget (mean of the final five evaluations, mean ± std over 5 seeds). Budget: ours / model-free arms. †At its converged, shorter budget. ‡With a hand-coded parameter prior. Bold: best mean; italic: mean at least the best mean minus the best arm's standard deviation, both computed before rounding.

F.2. Robustness of the score

Table 16 repeats Table 1 with the mean over the last $\min(5 \cdot 10^4, 25\%$ of the budget$)$ steps of each run instead of the final five evaluations. It is applied identically to every arm; the final-five score remains the primary metric (Section 4.1).

Task	HyLI (ours)	DLPA†	HyAR	P-DQN‡	HHQN	PA-TD3	H-PPO
Platform	**1.00 ± 0.00**	0.98 ± 0.03	0.97 ± 0.01	0.89 ± 0.03	0.44 ± 0.23	0.91 ± 0.08	0.80 ± 0.01
Goal	**0.76 ± 0.03**	0.57 ± 0.29	0.72 ± 0.02	0.61 ± 0.18	0.00 ± 0.00	0.00 ± 0.00	0.00 ± 0.00
Hard Goal	**0.78 ± 0.03**	0.34 ± 0.28	0.58 ± 0.08	0.06 ± 0.08	0.01 ± 0.02	0.18 ± 0.17	0.00 ± 0.00
Catch Point	*0.92 ± 0.03*	*0.92 ± 0.01*	0.72 ± 0.17	**0.92 ± 0.05**	0.31 ± 0.14	0.61 ± 0.14	0.70 ± 0.04
Hard Move (n=4)	0.92 ± 0.02	*0.95 ± 0.00*	**0.95 ± 0.01**	0.35 ± 0.05	0.63 ± 0.13	0.48 ± 0.21	0.65 ± 0.12
Hard Move (n=6)	**0.95 ± 0.02**	*0.94 ± 0.01*	0.93 ± 0.03	0.33 ± 0.06	0.18 ± 0.07	0.06 ± 0.03	0.57 ± 0.20
Hard Move (n=8)	**0.92 ± 0.02**	*0.92 ± 0.00*	0.86 ± 0.09	0.13 ± 0.03	0.05 ± 0.03	0.08 ± 0.02	0.15 ± 0.05

Table 16. Late-window mean (mean ± std over 5 seeds). Bold and italic as in Table 1.

Task	HyLI (ours)	DLPA†	HyAR	P-DQN‡	HHQN	PA-TD3	H-PPO
Platform	**0.98 ± 0.00**	0.96 ± 0.06	0.90 ± 0.02	0.87 ± 0.05	0.41 ± 0.10	0.88 ± 0.06	0.65 ± 0.02
Goal	**0.65 ± 0.02**	0.54 ± 0.27	0.59 ± 0.04	0.59 ± 0.15	0.00 ± 0.00	0.00 ± 0.00	0.00 ± 0.00
Hard Goal	**0.69 ± 0.02**	0.33 ± 0.27	0.46 ± 0.11	0.02 ± 0.03	0.02 ± 0.01	0.22 ± 0.15	0.00 ± 0.00
Catch Point	**0.90 ± 0.02**	0.92 ± 0.03	0.64 ± 0.12	0.84 ± 0.03	0.32 ± 0.05	0.39 ± 0.13	0.45 ± 0.02
Hard Move (n=4)	*0.87 ± 0.02*	0.94 ± 0.02	**0.88 ± 0.01**	0.33 ± 0.03	0.70 ± 0.08	0.24 ± 0.10	0.44 ± 0.08
Hard Move (n=6)	**0.89 ± 0.03**	0.93 ± 0.02	0.83 ± 0.03	0.27 ± 0.03	0.22 ± 0.08	0.05 ± 0.01	0.29 ± 0.09
Hard Move (n=8)	**0.84 ± 0.02**	0.88 ± 0.02	0.70 ± 0.04	0.08 ± 0.01	0.06 ± 0.02	0.07 ± 0.01	0.07 ± 0.01

Table 17. Area under the evaluation curve over our budget on the task, divided by its length (mean ± std over 5 seeds). Every arm is integrated over the same range. DLPA's runs end earlier; its curve is held at its last value to the end of the range, so its column is not comparable, is not ranked and is shown for completeness only. Held at its last value, DLPA would have the highest value on Catch Point, Hard Move (n=4), Hard Move (n=6) and Hard Move (n=8). HyAR's curve is integrated on its own step axis, without its pre-training. Bold and italic as in Table 1.

F.3. Sensitivity to the threshold

Task	thr.	HyLI (ours)	DLPA†	HyAR	P-DQN‡	HHQN	PA-TD3	H-PPO
Platform	75%	4k	**1k**	19.5k	5k	>200k (2/5)	17k	93k
	90%	4.5k	**1.5k**	25k	9k	>200k (2/5)	21.5k	>200k (0/5)
	100%	**5k**	8.5k	40k	47k	>200k (0/5)	27k	>200k (0/5)
Goal	75%	**32.5k**	20.5k (4/5)	60.3k	20.5k (4/5)	>300k (0/5)	>300k (0/5)	>300k (0/5)
	90%	**45k**	47k (4/5)	85.8k	31.5k (4/5)	>300k (0/5)	>300k (0/5)	>300k (0/5)
	100%	105k	73k (4/5)	**95.8k**	78.5k (4/5)	>300k (0/5)	>300k (0/5)	>300k (0/5)
Hard Goal	75%	**22k**	16.5k (3/5)	57.2k	>300k (0/5)	>300k (0/5)	>300k (2/5)	>300k (0/5)
	90%	**29.5k**	29k (3/5)	105k	>300k (0/5)	>300k (0/5)	>300k (2/5)	>300k (0/5)
	100%	**29.5k**	29k (3/5)	175k (4/5)	>300k (0/5)	>300k (0/5)	>300k (2/5)	>300k (0/5)
Catch Point	75%	15k	**7.5k**	174k	57.5k	>500k (0/5)	338k (4/5)	282k
	90%	20k	**10k**	221k	105k	>500k (0/5)	>500k (2/5)	432k (4/5)
	100%	30k	**17.5k**	256k (4/5)	135k	>500k (0/5)	>500k (0/5)	>500k (0/5)
Hard Move (n=4)	75%	15k	**5k**	185k	122k	32.5k	>500k (1/5)	268k (3/5)
	90%	27.5k	**15k**	185k	>500k (2/5)	55k	>500k (1/5)	>500k (2/5)
	100%	40k	**22.5k**	228k	>500k (0/5)	75k (4/5)	>500k (0/5)	>500k (0/5)
Hard Move (n=6)	75%	25k	**15k**	197k	228k	302k (3/5)	>500k (0/5)	415k (3/5)
	90%	35k	**22.5k**	212k	340k (4/5)	>500k (0/5)	>500k (0/5)	>500k (0/5)
	100%	60k	**37.5k**	265k	>500k (0/5)	>500k (0/5)	>500k (0/5)	>500k (0/5)
Hard Move (n=8)	75%	45k	**40k**	262k	>500k (0/5)	>500k (0/5)	>500k (0/5)	>500k (0/5)
	90%	62.5k	**47.5k**	275k	>500k (0/5)	>500k (0/5)	>500k (0/5)	>500k (0/5)
	100%	75k	**72.5k**	322k	>500k (0/5)	>500k (0/5)	>500k (0/5)	>500k (0/5)

Table 18. Total environment steps to 75%, 90% (Table 3) and 100% of HyAR's published final score; same conventions as Table 3, bold among the arms whose five seeds all reach the threshold. †At its converged, shorter budget. ‡With a hand-coded parameter prior. By this rule the rank of HyLI is the same at all three thresholds except on Platform (second at 75% and 90%, first at 100%) and Goal (first at 75% and 90%, second at 100%, behind HyAR).

F.4. Pareto view per task and on GPU

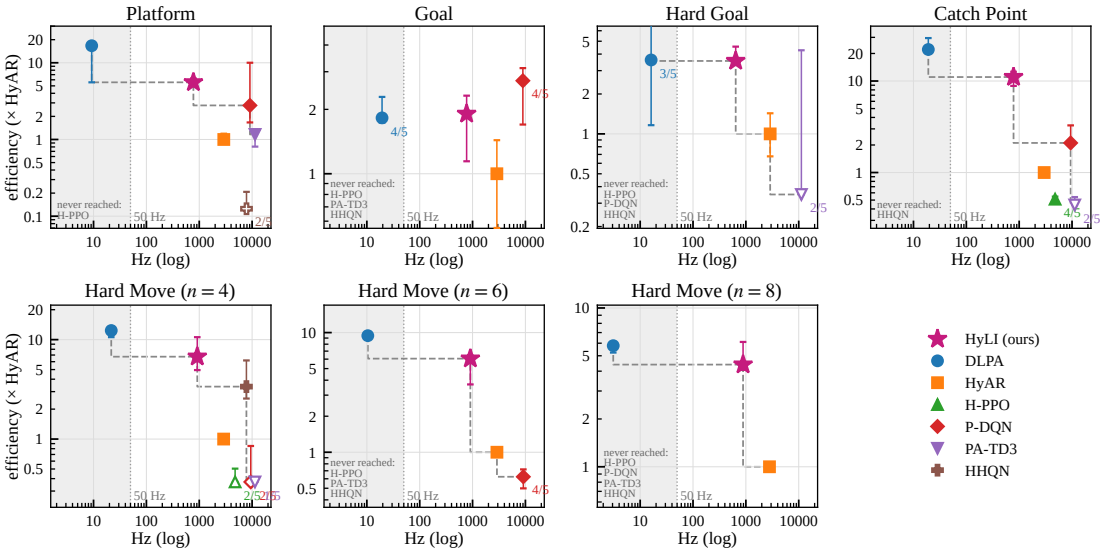


Figure 7. Figure 3 per task (CPU, one thread). Bars: inter-quartile range over seeds. Numbers next to a marker: seeds that reach the threshold, when fewer than five; arms that never reach it are listed in the panel.

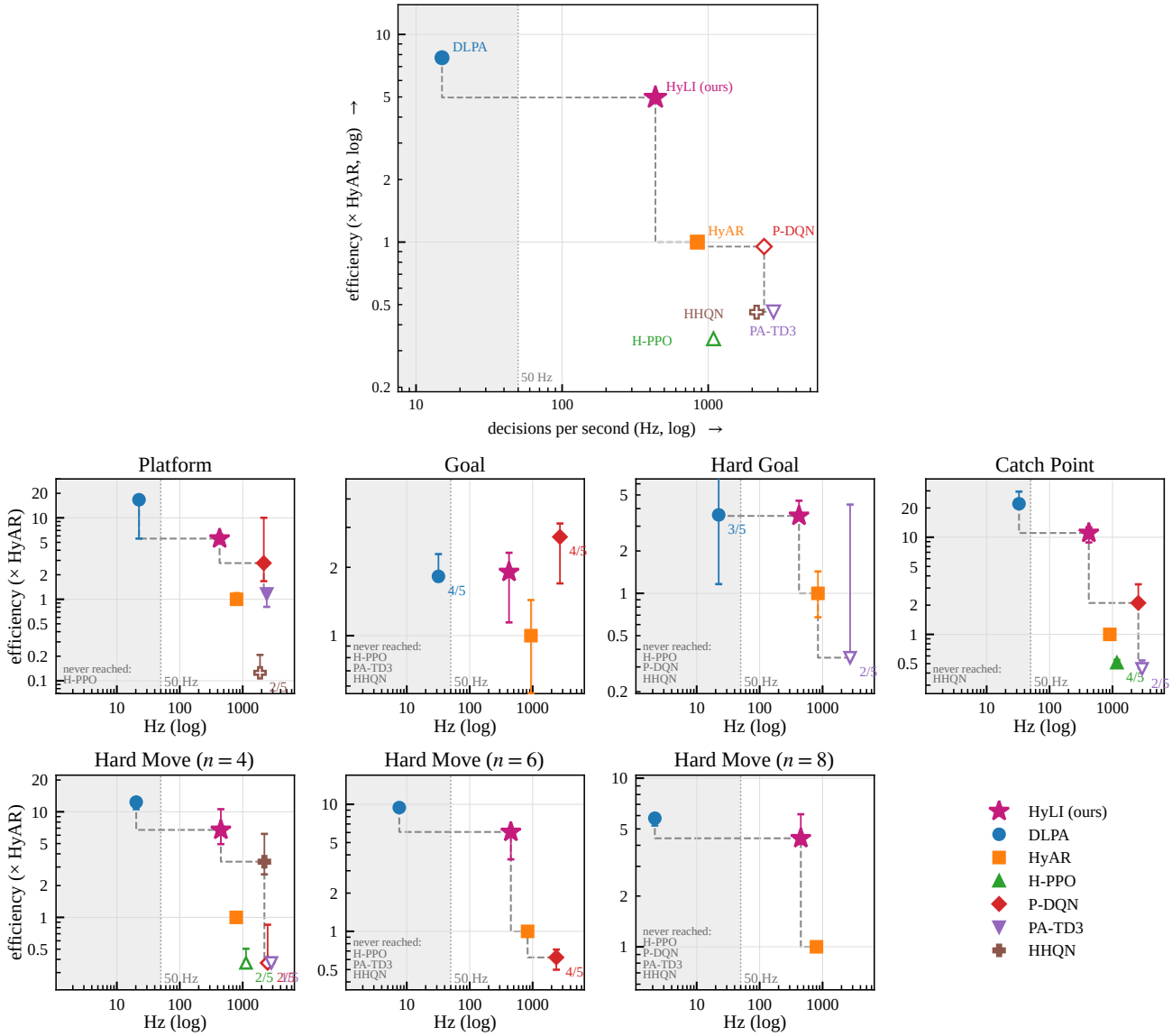


Figure 8. Figure 3 with latency measured on the GPU (RTX A4000, batch size 1). The shape is unchanged.

F.5. Latency on GPU and tail latency

Task	K	HyLI (ours)	DLPA	HyAR	P-DQN	HHQN	PA-TD3	H-PPO
CPU, 1 thread								
Platform	3	1.29 (1.31)	108 (109)	0.343 (0.346)	0.11 (0.111)	0.128 (0.13)	0.0879 (0.0888)	0.21 (0.212)
Goal	3	1.3 (1.32)	51.6 (51.8)	0.347 (0.349)	0.112 (0.113)	0.128 (0.129)	0.0886 (0.0921)	0.213 (0.223)
H. Goal	11	1.56 (1.59)	62 (62.4)	0.347 (0.35)	0.107 (0.108)	0.128 (0.129)	0.0891 (0.0929)	0.212 (0.214)
Catch	2	1.28 (1.3)	52.4 (52.6)	0.337 (0.341)	0.106 (0.108)	0.128 (0.13)	0.0889 (0.0933)	0.209 (0.211)
HM4	16	1.09 (1.11)	46.2 (46.5)	0.345 (0.348)	0.106 (0.107)	0.128 (0.129)	0.0883 (0.0895)	0.21 (0.212)
HM6	64	1.1 (1.12)	95.9 (98.2)	0.346 (0.356)	0.109 (0.11)	0.16 (0.161)	0.11 (0.113)	0.215 (0.218)
HM8	256	1.13 (1.15)	323 (332)	0.357 (0.363)	0.124 (0.129)	0.149 (0.15)	0.0968 (0.0976)	0.242 (0.246)
HM10	1024	1.29 (1.31)	1145 (1151)	0.381 (0.385)	0.222 (0.224)	0.249 (0.251)	0.164 (0.166)	0.358 (0.36)
GPU (NVIDIA RTX A4000)								
Platform	3	2.33 (2.38)	44.4 (45.6)	1.25 (1.29)	0.462 (0.481)	0.53 (0.566)	0.415 (0.425)	1.01 (1.69)
Goal	3	2.37 (2.6)	31.4 (39)	1.06 (1.17)	0.368 (0.377)	0.394 (0.403)	0.302 (0.312)	0.886 (0.912)
H. Goal	11	2.37 (2.68)	44.7 (45.5)	1.18 (1.31)	0.408 (0.427)	0.473 (0.484)	0.365 (0.375)	0.927 (0.964)
Catch	2	2.38 (2.71)	30.6 (30.8)	1.1 (1.28)	0.389 (0.398)	0.438 (0.447)	0.339 (0.348)	0.851 (0.875)
HM4	16	2.22 (2.58)	49.2 (49.7)	1.27 (1.31)	0.401 (0.409)	0.452 (0.461)	0.35 (0.356)	0.886 (0.909)
HM6	64	2.22 (2.55)	132 (133)	1.2 (1.32)	0.42 (0.432)	0.474 (0.486)	0.36 (0.37)	0.91 (0.935)
HM8	256	2.22 (2.4)	462 (464)	1.25 (1.4)	0.462 (0.469)	0.518 (0.527)	0.382 (0.399)	0.985 (1.02)
HM10	1024	2.21 (2.45)	1778 (1794)	1.24 (1.32)	0.576 (0.796)	0.562 (0.578)	0.429 (0.436)	0.928 (0.945)

Table 19. Milliseconds per decision, batch size 1, median (p90) over 1 000 decisions; CPU with one thread and GPU. At batch size 1 the GPU is slower than one CPU thread for every policy network.

F.6. Learning curves: full budgets, log axis and episode return

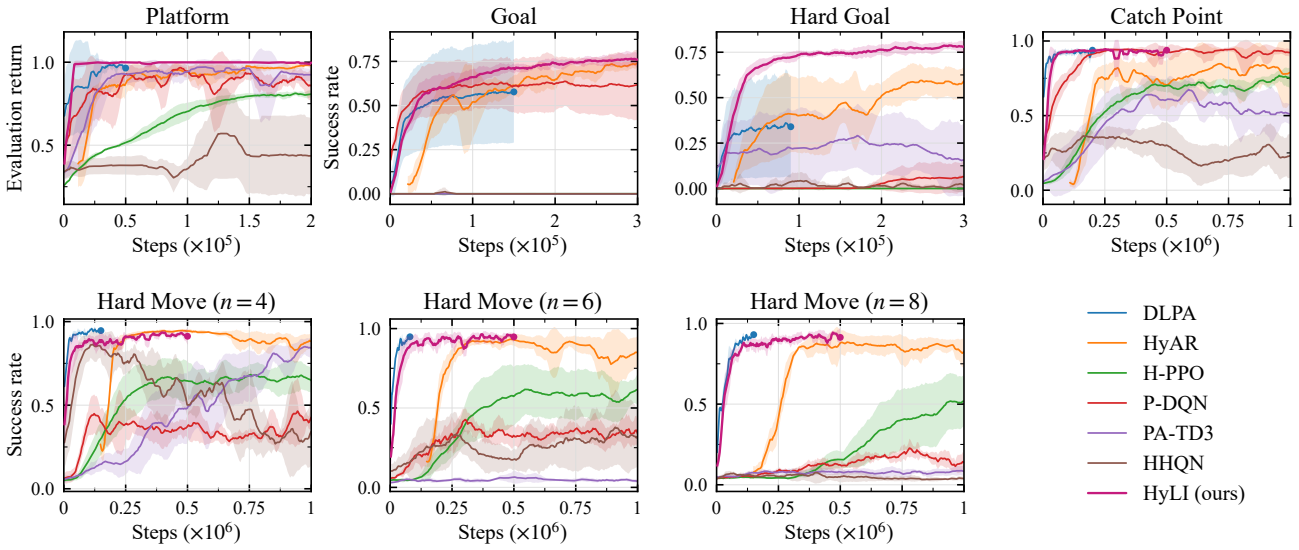


Figure 9. Figure 4 with every arm drawn over its full budget. As there, HyAR's reward-free pre-training steps are included on the step axis, so its curve starts later.

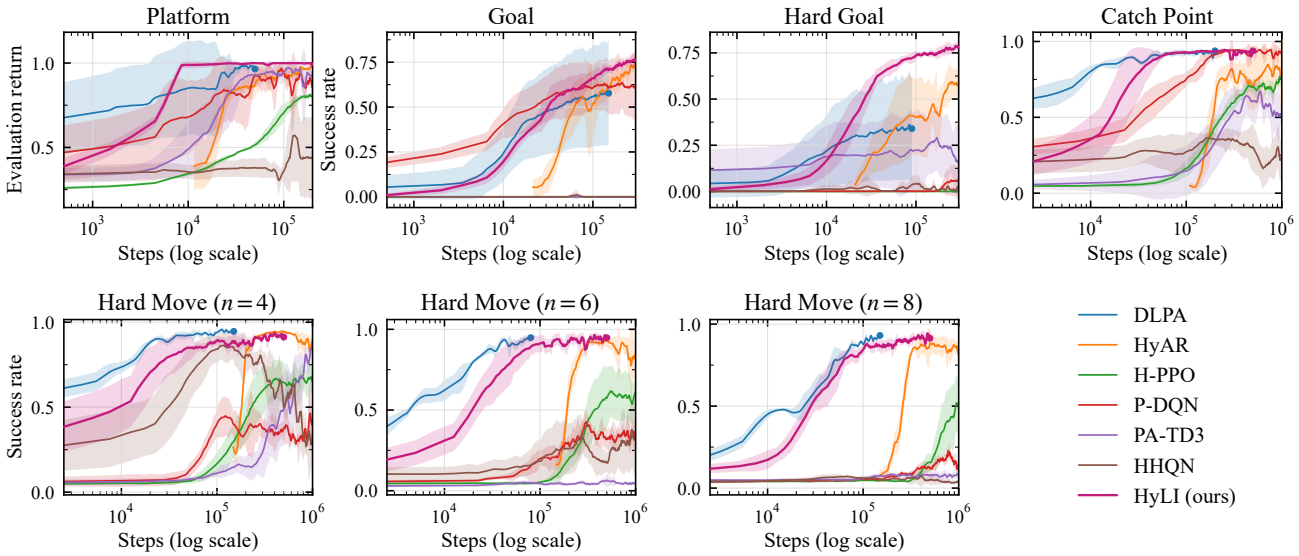


Figure 10. Figure 9 on a logarithmic step axis, which makes the short DLPA budgets readable. HyAR's pre-training steps are included on the step axis, as in Figure 4.

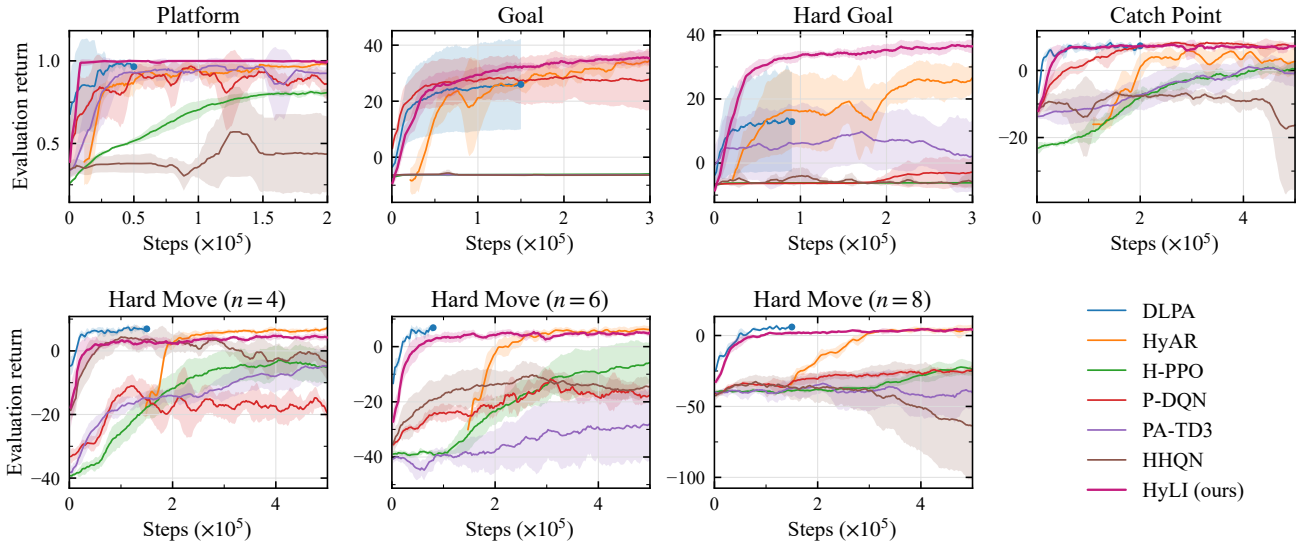


Figure 11. Figure 4 in evaluation episode return, the quantity plotted by Li et al. (2022) and Zhang et al. (2024). On Hard Move, HyAR's return lies above ours even where its success rate does not, because its successful episodes are shorter.

F.7. Budgets

Task	HyLI (ours)	DLPA†	HyAR	P-DQN‡	HHQN	PA-TD3	H-PPO
Platform	2e5	5e4	2e5°	2e5°	2e5°	2e5°	2e5°
Goal	3e5	1.5e5	3e5	3e5	3e5	3e5	3e5
Hard Goal	3e5	9e4	3e5	3e5	3e5	3e5	3e5
Catch Point	5e5	2e5	1e6	1e6	1e6	1e6	1e6
Hard Move (n=4)	5e5	1.5e5	1e6	1e6	1e6	1e6	1e6
Hard Move (n=6)	5e5	8e4	1e6	1e6	1e6	1e6	1e6
Hard Move (n=8)	5e5	1.5e5	1e6	1e6	1e6	1e6	1e6

Table 20. Budget of every cell in environment steps, as run (HyAR's excludes its pre-training). °: at least one seed's last evaluation lies before 99% of the budget.

F.8. Parameter heads

Task	Head	Head width	Score	IQM [95% CI]	Worst	Fail	Steps to thr.
Goal	sub*	default	$\mathbf{0.77 \pm 0.03}$	0.77 [0.74, 0.80]	0.74	0/5	45k
	multi	default	0.73 ± 0.03	0.72 [0.69, 0.77]	0.69	0/5	57.5k
	multi, param-matched	552	$\mathit{0.75 \pm 0.10}$	0.78 [0.62, 0.83]	0.57	0/5	45.5k (4/5)
Hard Goal	sub*	default	$\mathbf{0.79 \pm 0.04}$	0.80 [0.73, 0.82]	0.70	0/5	29.5k
	multi	default	$\mathit{0.77 \pm 0.03}$	0.77 [0.74, 0.81]	0.74	0/5	27.5k
	multi, param-matched	1225	$\mathit{0.77 \pm 0.04}$	0.76 [0.72, 0.81]	0.72	0/5	19.5k
Hard Move (n=4)	sub	default	$\mathit{0.90 \pm 0.03}$	0.91 [0.86, 0.93]	0.85	0/5	30k
	multi*	default	$\mathbf{0.91 \pm 0.05}$	0.93 [0.84, 0.95]	0.81	0/5	27.5k

Table 21. Parameter-head comparison of Figure 6: final score, mean $\pm$ std over 5 seeds (bold and italic as in Table 1; *: the head the method uses), inter-quartile mean, worst seed, failing seeds (final < 0.5) and median steps to 90% of HyAR's published score. Head width: hidden width of the parameter head (default: the MLP width of Table 6).

F.9. Ablation learning curves

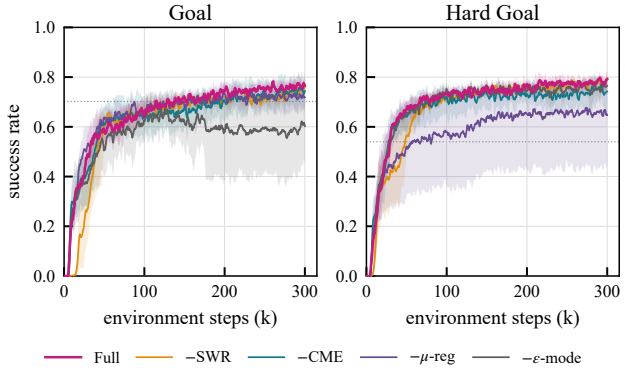


Figure 12. Leave-one-out ablation of Table 5: evaluation success rate, mean over 5 seeds with a 95% pointwise bootstrap band.

G. Hardware and compute

Hardware. Every run used one of several identical workstations: one NVIDIA RTX A4000, an Intel x86-64 CPU with 20 logical cores and 64 GB of RAM. Each seed ran as its own process with one PyTorch CPU thread. Latency (Section 4.2) was measured on one of these machines, on the CPU with one thread and on the GPU.

Compute. Up to five seeds shared one GPU. A seed of ours took tens of hours; a seed of DLPA took tens to hundreds of hours at budgets 2 to 6$\times$ shorter than ours, because it plans at every training step; the model-free arms took between one and a few tens of hours. Wall clock depended on how many processes shared a machine, so we do not compare arms by it; the controlled measurements are the update time (Table 7) and the decision time (Table 2).